© 2022. Published by The Company of Biologists Ltd | Development (2022) 149, dev200667. doi:10.1242/dev.200667

RESEARCH ARTICLE

The transcription factors Foxf1 and Foxf2 integrate the SHH, HGF and TGFβ signaling pathways to drive tongue organogenesis

Jingyue Xu[1], Han Liu[1], Yu Lan[1,2,3] and Rulang Jiang[1,2,3,*]

ABSTRACT

The tongue is a highly specialized muscular organ with diverse cellular origins, which provides an excellent model for understanding mechanisms controlling tissue-tissue interactions during organogenesis. Previous studies showed that SHH signaling is required for tongue morphogenesis and tongue muscle organization, but little is known about the underlying mechanisms. Here we demonstrate that the Foxf1/Foxf2 transcription factors act in the cranial neural crest cell (CNCC)-derived mandibular mesenchyme to control myoblast migration into the tongue primordium during tongue initiation, and thereafter continue to regulate intrinsic tongue muscle assembly and lingual tendon formation. We performed chromatin immunoprecipitation sequencing analysis and identified *Hgf*, *Tgfb2* and *Tgfb3* among the target genes of Foxf2 in the embryonic tongue. Through genetic analyses of mice with CNCC-specific inactivation of *Smo* or both *Foxf1* and *Foxf2*, we show that Foxf1 and Foxf2 mediate hedgehog signaling-mediated regulation of myoblast migration during tongue initiation and intrinsic tongue muscle formation by regulating the activation of the HGF and TGFβ signaling pathways. These data uncover the molecular network integrating the SHH, HGF and TGFβ signaling pathways in regulating tongue organogenesis.

KEY WORDS: SHH, Gene regulatory network, Myoblast migration, Neural crest, TGFβ signaling, Tongue development

INTRODUCTION

The mammalian tongue is a specialized muscular organ that performs multiple essential functions including mastication, deglutition, oral sensation, oral cleansing, airway maintenance and vocalization (Iwasaki, 2002). The cells that perform these functions have diverse embryonic origins, including the oral ectoderm, cranial neural crest cells (CNCCs) and the paraxial mesoderm (Kapsimali and Barlow, 2013; Parada et al., 2012). Tongue development is initiated by the formation of a medial triangular elevation on top of the first (mandibular) arch called the median lingual swelling. In mouse, at around embryonic (E) day 10.5, a pair of lateral lingual swellings form on the oral side of the mandibular arch and subsequently fuse with the medial lingual swelling. These lingual swellings from the mandibular arch form the anterior two-thirds of the tongue. Two outgrowths arise from the third and fourth branchial arches, known as the copula and the hypopharyngeal eminence, which form the primordium for the posterior third of the tongue. The initial tongue outgrowths develop through interactions between the oropharyngeal epithelium and the underlying CNCC-derived mesenchyme. At the same developmental stage (around E10.5), the myogenic progenitor cells delaminate from caudal occipital somites and migrate along the hypoglossal cord to the mandibular arch, and subsequently populate the tongue primordium. Reciprocal interactions among CNCCs, myogenic cells and oral epithelial cells play an essential role in regulating tongue development. As development proceeds, the myogenic progenitor cells receive signals from neighboring cells (e.g. CNCCs), withdraw from the cell cycle to become myocytes and fuse to form multinucleated myotubes (reviewed by Cobourne et al., 2019; Parada and Chai, 2015; Parada et al., 2012). By E13.5, the major muscular structures of the tongue are clearly discernable. The tongue is divided into bilateral halves by the CNCC-derived midline fibrous septum, called the lingual septum, symmetrically arranged intrinsic muscles and a specialized group of extrinsic muscles (Parada et al., 2012). The extrinsic muscles consist of the paired hyoglossus, genioglossus, styloglossus and palatoglossus muscles, which attach to the hyoid bone, mandible, base of skull and soft palate, respectively. The intrinsic muscles include the superior and inferior longitudinal, transverse and vertical muscles, which control the shape of the tongue dorsum in three dimensions (Parada et al., 2012). The coordination of the muscle movement is supported by the CNCC-derived midline lingual septum and peripheral aponeurosis within the tongue dorsum. Although tongue anatomy has been illustrated for many years, the molecular mechanisms controlling tongue development and morphogenesis are still largely unresolved (Cobourne et al., 2019; Parada et al., 2012).

Hedgehog signaling plays essential roles in multiple developmental processes in vertebrates (Briscoe, 2009; Ericson et al., 1997; Ingham and McMahon, 2001; McMahon et al., 2003; Riddle et al., 1993; Tickle and Towers, 2017). Sonic hedgehog (SHH), expressed by the pharyngeal endoderm, is crucial for the survival and proliferation of the CNCCs colonizing the mandibular arch (Brito et al., 2006; Haworth et al., 2007; Jeong et al., 2004; Xu et al., 2019). The expression of *Shh* is maintained in the epithelium of the primordial tongue and becomes restricted to fungiform papillae of the anterior tongue by E12.5 (Jung et al., 1999). Tissue-specific inactivation of *Shh* in the early oropharyngeal epithelium resulted in aglossia and micrognathia (Billmyre and Klingensmith, 2015). Tissue-specific inactivation of *Smo*, which encodes an obligatory transducer of hedgehog signaling (Briscoe and Vincent, 2013; Jeong et al., 2004; Zhang et al., 2001), in all neural crest cells or specifically in the CNCC-derived mandibular arch mesenchyme also caused tongue agenesis (Jeong et al., 2004; Xu et al., 2019). Furthermore, Okuhara et al. (2019) showed that the $Shh^{MFCS4/-}$ mouse embryos with severely decreased *Shh* expression in the developing tongue epithelium exhibited disruption of both intrinsic

[1]Division of Developmental Biology, Cincinnati Children's Hospital Medical Center, Cincinnati, OH 45229, USA. [2]Division of Plastic Surgery, Cincinnati Children's Hospital Medical Center, Cincinnati, OH 45229, USA. [3]Departments of Pediatrics and Surgery, University of Cincinnati College of Medicine, Cincinnati, OH 45229, USA.

*Author for correspondence (Rulang.Jiang@cchmc.org)

R.J., 0000-0001-7842-4696

Handling Editor: Liz Robertson
Received 20 February 2022; Accepted 26 September 2022

Development (2022) 149, dev200667. doi:10.1242/dev.200667

tongue muscle organization and lingual septum tendon formation (Okuhara et al., 2019). In addition, temporally induced global *Shh* gene inactivation at E10.5 in mouse embryos did not affect initial myoblast migration to the tongue primordium but caused significant disorganization of the intrinsic muscles and disruption of tendon marker gene expression in the tongue (Okuhara et al., 2019). Taken together, these results indicate an essential role for SHH-Smo signaling activity in CNCCs in regulating tongue myogenesis and tongue muscle organization. However, the molecular mechanism mediating the function of SHH signaling in the regulation of myoblast migration and lingual tendon formation is still unknown.

The forkhead box (Fox) family proteins form a large family of DNA-binding transcription factors (Clark et al., 1993; Kaufmann and Knöchel, 1996). It has been shown that hedgehog signaling is required for the expression of several Fox family genes, including *Foxc2*, *Foxd1*, *Foxd2*, *Foxf1* and *Foxf2*, in the CNCC-derived facial mesenchyme (Jeong et al., 2004). Foxf1 and Foxf2 share highly conserved amino acid sequences in the forkhead DNA-binding domain (100% identical between Foxf1 and Foxf2 in mouse and 97% identical between FOXF1 and FOXF2 in human) (Hellqvist et al., 1998, 1996; Mahlapuu et al., 1998). We recently demonstrated that hedgehog signaling acts through the Foxf1/Foxf2 transcription factors to pattern the oral-aboral axis of the CNCC-derived mandibular mesenchyme (Xu et al., 2019). In this study, we show that hedgehog-Foxf1/Foxf2 signaling in the CNCC-derived mesenchyme activates HGF expression to direct the migration of myoblasts into the tongue primordium during tongue initiation, and regulates lingual tendon development and tongue muscle morphogenesis through activation of TGFβ signaling.

RESULTS

Foxf1 and Foxf2 act cell non-autonomously in the CNCC-derived tongue mesenchyme to regulate intrinsic tongue muscle formation

To elucidate the function of Foxf1 and Foxf2 in tongue development, we examined the patterns of expression of Foxf1 and Foxf2 in the developing mouse tongue by immunofluorescence staining. We found that both Foxf1 and Foxf2 were expressed mainly in the CNCC-derived tongue mesenchyme and were largely excluded from the myogenic cells marked by high levels of muscle actin expression (Fig. 1). Among the CNCC-derived tissues in the developing tongue, tendons and ligaments not only serve as a scaffold, but also play important roles in guiding the differentiation and morphogenesis of the tongue muscles (Nassari et al., 2017; Parada and Chai, 2015). To better understand the roles of Foxf1 and Foxf2 in tongue development, we compared their expression patterns with those of Scx-GFP, a transgenic green fluorescent protein reporter specifically expressed throughout the tendon lineages (Pryce et al., 2007) (Fig. 1B,E,H,K). From E12.5 to E13.5, the Scx-GFP+ cells in the developing tongue condensed to form the fibrous lingual septum tendon at the midline and the submucosal lingual aponeurosis, as the lingual myoblasts differentiate and organize into discrete intrinsic muscles (Fig. 1). By E13.5, frontal sections of the tongue clearly showed that the

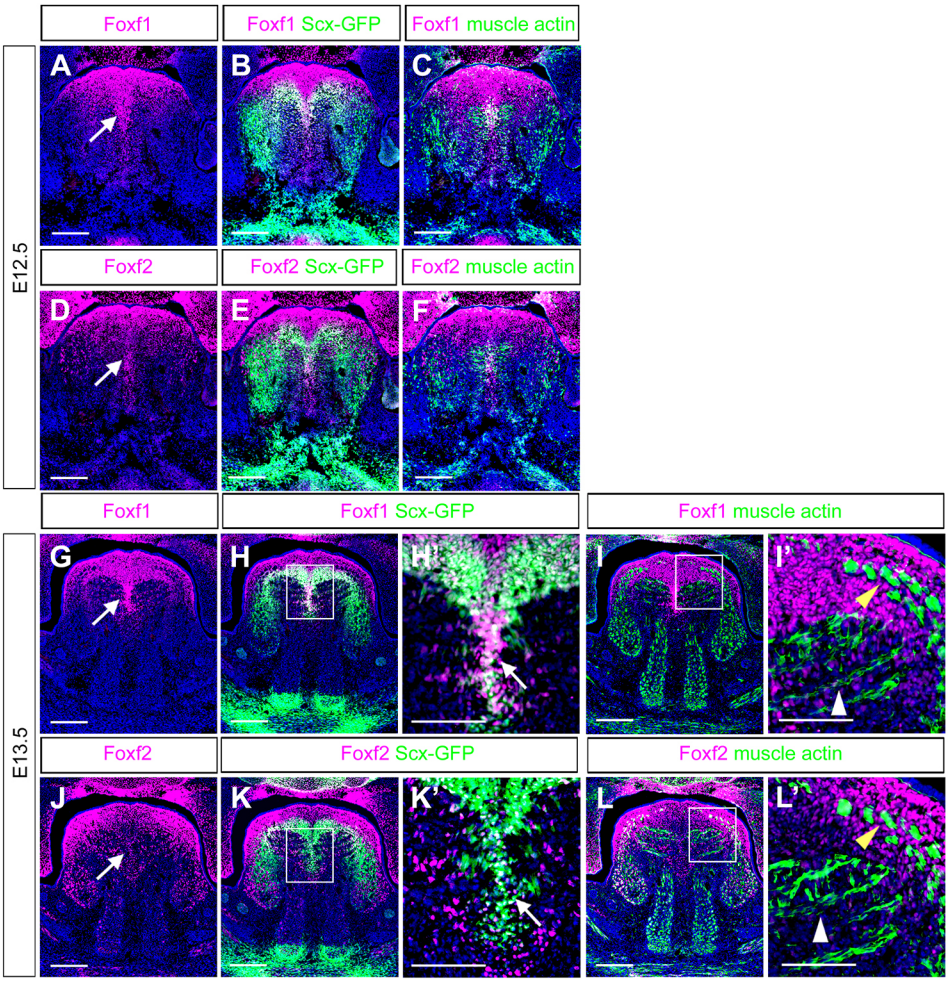

Fig. 1. Expression of Foxf1 and Foxf2 during tongue development. (A-L′) Frontal sections through the developing tongue in E12.5 (A-F) and E13.5 (G-L′) mouse embryos showing immunofluorescence detection of Foxf1 (A-C,G-I′, magenta), Foxf2 (D-F,J-L′, magenta), muscle actin (C,F,I,I′,L,L′, green) and Scx-GFP (B,E,H,H′,K,K′, green). Panels H′ and K′ show higher-magnification views of the boxed areas in H and K, respectively, revealing the substantial overlap of Foxf1 and Foxf2 with Scx-GFP in the developing lingual septum. Panels I′ and L′ show higher magnification views of the boxed areas in I and L, respectively, showing that there was little Foxf1 and Foxf2 expression in the muscle actin-positive muscle bundles. Arrows point to the developing midline lingual septum. White arrowheads point to the transverse muscle. Yellow arrowheads point to the superior longitudinal muscle. Images are representative of three embryos. Scale bars: 200 µm (A-L); 100 µm (H′-L′).

Development (2022) 149, dev200667. doi:10.1242/dev.200667

transverse muscles extend from the lingual septum tendon at the midline to the lateral fibrous submucosa (Fig. 1I,I′,L,L′). We found that the expression of both Foxf1 and Foxf2 partly overlapped with that of Scx-GFP at E12.5 and E13.5 (Fig. 1B,E,H,H′,K,K′). Whereas the expression of Foxf2 extended to more lateral regions of the developing tongue, the expression of Foxf1 was stronger in Scx-GFP+ cells forming the lingual septum tendon and the dorsal lingual aponeurosis (Fig. 1G,H,H′, compare with Fig. 1J,K,K′).

As mouse embryos lacking Foxf1 function die during mid-gestation due to defects in extraembryonic mesoderm development (Mahlapuu et al., 2001), we investigated whether Foxf1 is required in the neural crest-derived craniofacial mesenchyme for tongue organogenesis using Cre/loxP-mediated tissue-specific gene inactivation. Mice with tissue-specific inactivation of *Foxf1* in premigratory CNCCs (*Foxf1*$^{c/c}$*Wnt1-Cre*) exhibited a cleft palate (*n*=9) (Fig. S1A,B) and a variable tongue phenotype ranging from an obviously smaller tongue lacking the Scx+ midline septum tendon (2/9) to moderately reduced tongue size (3/9) to a largely normal-looking tongue (4/9) (Fig. S1C-F). Whereas *Foxf2*$^{c/c}$*Wnt1-Cre* mice also had a cleft palate defect and the tongue was partly wedged between the palatal shelves in frontal sections (Fig. S2), the tongue muscle organization and tongue size in *Foxf2*$^{c/c}$*Wnt1-Cre* embryos (*n*=5) appeared comparable with those of control littermates (*n*=13) (Fig. S2).

As *Foxf1* and *Foxf2* exhibit partly overlapping patterns of expression in the developing tongue (Fig. 1), and as *Foxf1*$^{c/c}$*Foxf2*$^{c/c}$*Wnt1-Cre* embryos had tongue agenesis (Xu et al., 2019), we next examined tongue development in the *Foxf1*$^{c/c}$*Foxf2*$^{c/+}$*Wnt1-Cre* and *Foxf1*$^{c/+}$*Foxf2*$^{c/c}$*Wnt1-Cre* mice. At postnatal (P) day 0, the *Foxf1*$^{c/c}$*Foxf2*$^{c/+}$*Wnt1-Cre* mice exhibited shortened mandibles compared with those of control littermates (Fig. S3A-C). Quantitative measurement of the length of the mandibular bone showed significant reduction in the length of the mandible in *Foxf1*$^{c/c}$*Foxf2*$^{c/+}$*Wnt1-Cre* mice compared with that of control littermates, whereas the mandible bone length in the *Foxf1*$^{c/+}$*Foxf2*$^{c/c}$*Wnt1-Cre* mice was similar to that of control littermates (Fig. S3D-H). In addition, the *Foxf1*$^{c/c}$*Foxf2*$^{c/+}$*Wnt1-Cre* mice exhibited deficiency in the molar alveolar bone (Fig. S3E). All *Foxf1*$^{c/c}$*Foxf2*$^{c/+}$*Wnt1-Cre* embryos exhibited narrower and shortened tongues that lacked the Scx+ midline lingual septum tendon, compared with those of control littermates at E16.5 (*n*=6) (Fig. 2A,B), whereas the tongues in the E16.5 *Foxf1*$^{c/+}$*Foxf2*$^{c/c}$*Wnt1-Cre* embryos appeared slightly reduced in width and length (*n*=7) (Fig. 2C). At E14.5, although control embryos showed well-organized intrinsic and extrinsic tongue muscles (Fig. 2D,G,J), *Foxf1*$^{c/c}$*Foxf2*$^{c/+}$*Wnt1-Cre* embryos exhibited absence of most of the transverse muscles and severely hypoplastic vertical muscles, as well as thickened but disorganized superior longitudinal muscles of the tongue (Fig. 2E,H). The *Foxf1*$^{c/+}$*Foxf2*$^{c/c}$*Wnt1-Cre* embryonic tongue also displayed reduced and disorganized transverse and vertical muscles (Fig. 2F,I). Whereas all four pairs of extrinsic tongue muscles could be identified in control, *Foxf1*$^{c/c}$*Foxf2*$^{c/+}$*Wnt1-Cre* and *Foxf1*$^{c/+}$*Foxf2*$^{c/c}$*Wnt1-Cre* embryos (Fig. 2G-L), the palatoglossus and styloglossus muscles were disorganized in the posterior region of the tongue in the *Foxf1*$^{c/c}$*Foxf2*$^{c/+}$*Wnt1-Cre* embryos (Fig. 2K, compare with Fig. 2J).

We then examined whether the migration and differentiation of myogenic progenitor cells were affected at earlier stages in the *Foxf1*$^{c/c}$*Foxf2*$^{c/+}$*Wnt1-Cre* and *Foxf1*$^{c/+}$*Foxf2*$^{c/c}$*Wnt1-Cre* embryos. At E12.5, MyoD (Myod1)-positive myogenic progenitor cells populated the tongue primordium in control,

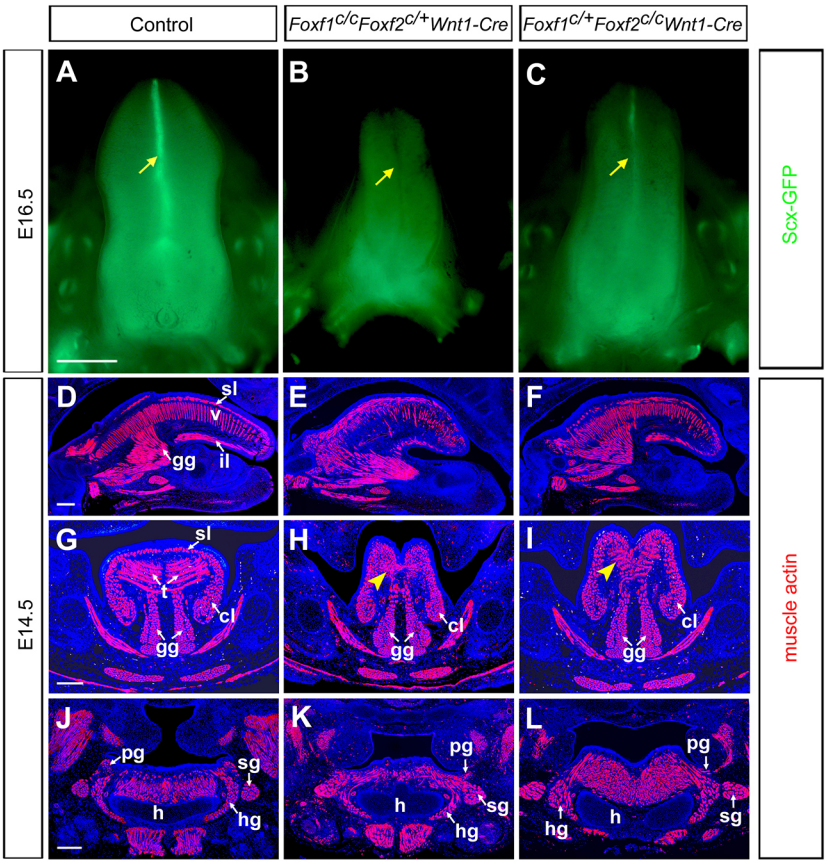

Fig. 2. *Foxf1*$^{c/c}$*Foxf2*$^{c/+}$*Wnt1-Cre* and *Foxf1*$^{c/+}$*Foxf2*$^{c/c}$*Wnt1-Cre* mutant mice exhibit defects in the intrinsic tongue muscles. (A-C) Whole-mount view of E16.5 control (A) (*n*=17), *Foxf1*$^{c/c}$*Foxf2*$^{c/+}$*Wnt1-Cre* (B) (*n*=6) and *Foxf1*$^{c/+}$*Foxf2*$^{c/c}$*Wnt1-Cre* (C) (*n*=7) embryonic tongues showing the patterns of green fluorescence from the Scx-GFP transgenic reporter. Yellow arrows point to the location of the lingual septum tendon in the tongue. (D-L) Sagittal (*n*=3 for each genotype) (D-F) and frontal (*n*=3 for each genotype) (G-L) sections through the tongues of E14.5 control (D,G,J), *Foxf1*$^{c/c}$*Foxf2*$^{c/+}$*Wnt1-Cre* (E,H,K) and *Foxf1*$^{c/+}$*Foxf2*$^{c/c}$*Wnt1-Cre* (F,I,L) embryos showing immunofluorescence detection of muscle actin (red). cl, combined longitudinal muscle (including hg and sg); gg, genioglossus muscle; h, hyoid bone; hg, hyoglossus muscle; il, inferior longitudinal muscle; pg, palatoglossus muscle; sg, styloglossus muscle; sl, superior longitudinal muscle; t, transverse muscle; v, vertical muscle. Yellow arrowheads point to the location of the transverse and vertical muscles in the tongue. Scale bars: 1000 µm (A-C); 200 µm (D-L).

Development (2022) 149, dev200667. doi:10.1242/dev.200667

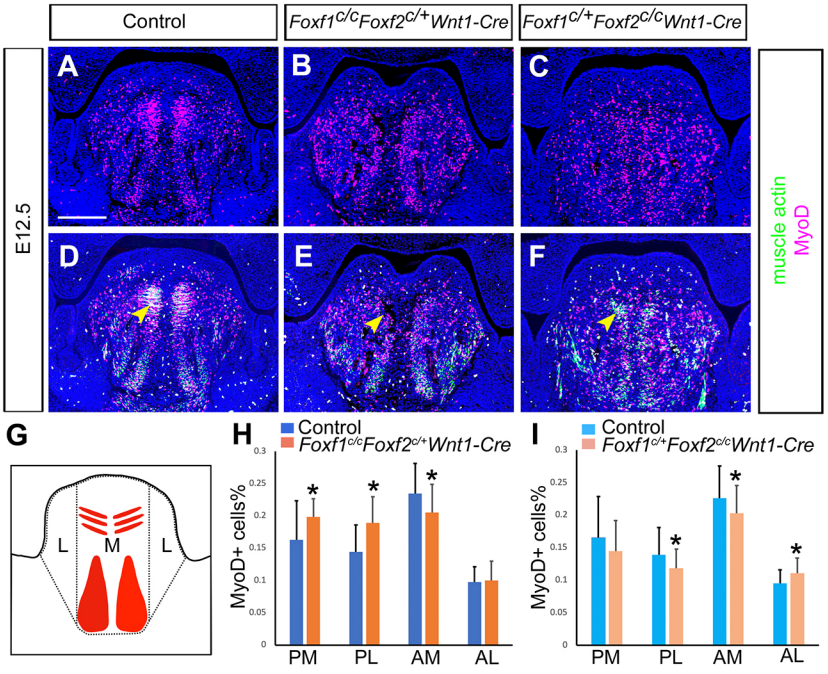

Fig. 3. *Foxf1*$^{c/c}$*Foxf2*$^{c/+}$*Wnt1-Cre* and *Foxf1*$^{c/+}$*Foxf2*$^{c/c}$*Wnt1-Cre* mutant mice exhibit defects in tongue myogenesis. (A-F) Frontal sections through the developing tongue in E12.5 control (A,D) (*n*=7), *Foxf1*$^{c/c}$*Foxf2*$^{c/+}$*Wnt1-Cre* (B,E) (*n*=4) and *Foxf1*$^{c/+}$*Foxf2*$^{c/c}$*Wnt1-Cre* (C,F) (*n*=4) embryos showing patterns of immunofluorescence staining of muscle actin (green) and MyoD (magenta). Yellow arrowheads in D-F point to the myogenic progenitor cells of transverse and vertical muscles of the tongue. (G-I) Quantification of the percentage of MyoD-positive nuclei in the anterior versus posterior and medial versus lateral domains of tongue mesenchyme (L, lateral; M, medial), depicted by the schematic in G. Statistical analysis was performed on data from five control embryos (63 sections for the posterior tongue and 66 sections for the anterior tongue) and four *Foxf1*$^{c/c}$*Foxf2*$^{c/+}$*Wnt1-Cre* (49 sections for the posterior tongue and 49 sections for the anterior tongue) embryos (H), or on data from four control embryos (51 sections for the posterior tongue and 50 sections for the anterior tongue) and four *Foxf1*$^{c/+}$*Foxf2*$^{c/c}$*Wnt1-Cre* embryos (42 sections for the posterior tongue and 42 sections for the anterior tongue) (I). Statistical significance was determined by a two-tailed unpaired Student's *t*-test using Excel. The results are presented as mean±s.d. AL, anterior lateral; AM, anterior medial; PL, posterior lateral; PM, posterior medial. **P*<0.05. Scale bar: 200 µm.

Foxf1$^{c/c}$*Foxf2*$^{c/+}$*Wnt1-Cre* and *Foxf1*$^{c/+}$*Foxf2*$^{c/c}$*Wnt1-Cre* embryos (Fig. 3A-C). However, although control embryos exhibited formation of muscle actin-positive transverse and vertical muscle bundles (Fig. 3D), few muscle actin-positive myocytes were detected in the corresponding regions of the developing tongue in the *Foxf1*$^{c/c}$*Foxf2*$^{c/+}$*Wnt1-Cre* embryos (Fig. 3E), and the formation of the transverse and vertical muscle bundles was also impaired in the *Foxf1*$^{c/+}$*Foxf2*$^{c/c}$*Wnt1-Cre* embryonic tongue (Fig. 3F). We compared the amount and regional distribution of MyoD+ myoblast cells in the developing tongue at E12.5 in control, *Foxf1*$^{c/c}$*Foxf2*$^{c/+}$*Wnt1-Cre* and *Foxf1*$^{c/+}$*Foxf2*$^{c/c}$*Wnt1-Cre* embryos to better understand the defect in tongue muscle formation in the mutant embryos. In comparison with control littermates, the *Foxf1*$^{c/c}$*Foxf2*$^{c/+}$*Wnt1-Cre* embryos exhibited increased proportion of myoblast cells in the posterior half of the tongue and a significant decrease in the number of myoblasts in the medial region of the anterior tongue (Fig. 3G,H) whereas the *Foxf1*$^{c/+}$*Foxf2*$^{c/c}$*Wnt1-Cre* embryos had slightly reduced numbers of myoblasts in the lateral regions of the posterior as well as in the medial region of the anterior tongue but an increased number of myoblasts in the lateral regions of the anterior tongue (Fig. 3I). The disruption of intrinsic tongue muscle formation in the *Foxf1*$^{c/c}$*Foxf2*$^{c/+}$*Wnt1-Cre* and *Foxf1*$^{c/+}$*Foxf2*$^{c/c}$*Wnt1-Cre* embryos correlated with the patterns of Foxf1 and Foxf2 expression in the developing tongue, indicating that Foxf1 and Foxf2 in the CNCC-derived tongue mesenchyme play an important cell non-autonomous role in regulating intrinsic muscle formation.

As Foxf1 and Foxf2 have been shown to act downstream of SHH signaling to pattern the oral-aboral axis of the distal mandibular arch by antagonizing BMP signaling (Xu et al., 2019), we analyzed whether the *Foxf1*$^{c/c}$*Foxf2*$^{c/+}$*Wnt1-Cre* and *Foxf1*$^{c/+}$*Foxf2*$^{c/c}$*Wnt1-Cre* embryos had aberrantly expanded expression of the BMP target genes *Msx1* and *Msx2* in the developing mandibular arches. In comparison with their control littermates at E10.5, the *Foxf1*$^{c/c}$*Foxf2*$^{c/+}$*Wnt1-Cre* embryos, but not the *Foxf1*$^{c/+}$*Foxf2*$^{c/c}$*Wnt1-Cre* embryos, exhibited expanded expression of *Msx1* and *Msx2* mRNAs to the oral side of the most distal region of the mandibular arch (Fig. S3I-N). However, in contrast to the *Foxf1*$^{c/c}$*Foxf2*$^{c/c}$*Wnt1-Cre* embryos, in which the disruption of the oral-aboral patterning of the early mandibular arches resulted in partial duplication of the mandibular dentary bone at the oral side at the expanse of tongue formation (Xu et al., 2019), the *Foxf1*$^{c/c}$*Foxf2*$^{c/+}$*Wnt1-Cre* embryos had no ectopic ossification in the mandibular mesenchyme, but exhibited a significantly reduced mandible (Fig. S3A,B,D,E) and tongue size at later developmental stages (Fig. 2). These results indicate that the expanded BMP signaling in the distal mandibular arches did not result in overt disruption of oral-aboral patterning of mandibular structures, but likely contributed to the more dramatic tongue defects in the *Foxf1*$^{c/c}$*Foxf2*$^{c/+}$*Wnt1-Cre* embryos than in the *Foxf1*$^{c/+}$*Foxf2*$^{c/c}$*Wnt1-Cre* embryos.

Foxf1 and Foxf2 function in the formation of lingual septum tendon

To understand how the function of Foxf1 and Foxf2 in the CNCC-derived tongue mesenchyme affects tongue myogenesis, we analyzed tongue tendon formation in the *Foxf1*$^{c/c}$*Foxf2*$^{c/+}$*Wnt1-Cre* and *Foxf1*$^{c/+}$*Foxf2*$^{c/c}$*Wnt1-Cre* embryos. By E13.5, Scx-GFP clearly labeled the lingual septum tendon in control embryos (Fig. 4A). However, the *Foxf1*$^{c/c}$*Foxf2*$^{c/+}$*Wnt1-Cre* embryos lacked the Scx-GFP positive lingual septum tendon (Fig. 4B), whereas the *Foxf1*$^{c/+}$*Foxf2*$^{c/c}$*Wnt1-Cre* embryos displayed lingual septum tendon with decreased and often disrupted Scx-GFP expression (Fig. 4C). Immunofluorescence labeling of frontal sections showed that the muscle actin-positive transverse muscles were connected to the Scx-GFP-positive lingual septum tendon at the midline in control embryos (Fig. 4D,G), whereas both the Scx-GFP-positive lingual septum tendon and muscle actin-positive transverse muscles were absent in the E13.5 *Foxf1*$^{c/c}$*Foxf2*$^{c/+}$*Wnt1-Cre* mutant tongue (Fig. 4E,H). Scx-GFP-positive cells in the dorsal submucosal lingual aponeurosis were less condensed and mixed with muscle actin-positive myogenic cells in the E13.5 *Foxf1*$^{c/c}$*Foxf2*$^{c/+}$*Wnt1-Cre* mutant tongue compared with those in control embryos (Fig. 4D,E,G,H).

Development (2022) 149, dev200667. doi:10.1242/dev.200667

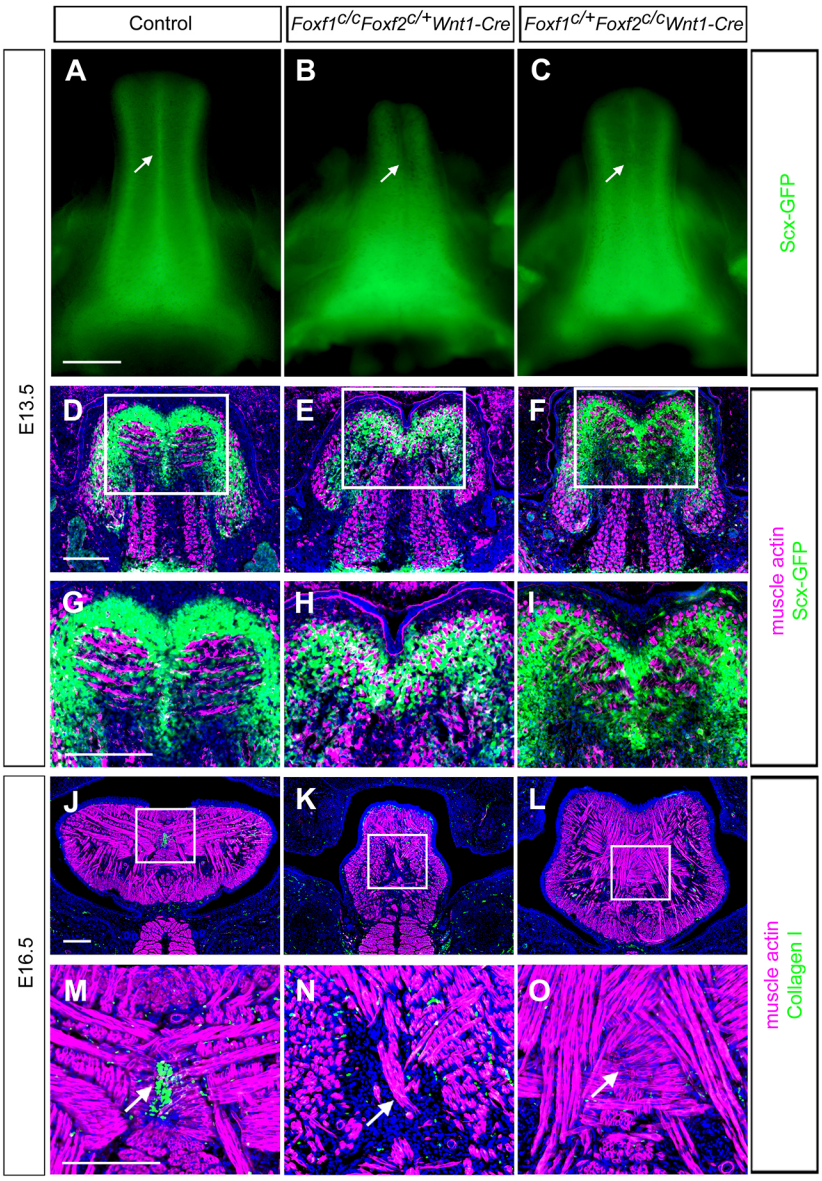

Fig. 4. *Foxf1$^{c/c}$Foxf2$^{c/+}$Wnt1-Cre* and *Foxf1$^{c/+}$Foxf2$^{c/c}$Wnt1-Cre* mutant mice exhibit defects in lingual septum tendon formation. (A-C) Whole-mount view of E13.5 control (A), *Foxf1$^{c/c}$Foxf2$^{c/+}$Wnt1-Cre* (B) and *Foxf1$^{c/+}$Foxf2$^{c/c}$Wnt1-Cre* (C) embryonic tongues to visualize the patterns of green fluorescence from the Scx-GFP transgenic reporter (*n*=3 for each genotype). Arrows point to the location of the lingual septum tendon in the tongue. (D-I) Frontal sections through the developing tongue in E13.5 control (D,G), *Foxf1$^{c/c}$Foxf2$^{c/+}$Wnt1-Cre* (E,H) and *Foxf1$^{c/+}$Foxf2$^{c/c}$Wnt1-Cre* (F,I) embryos showing the patterns of Scx-GFP (green) and immunostaining of muscle actin (magenta). Higher-magnification views of the boxed areas in D-F are shown in G-I, respectively. (J-O) Frontal sections through the developing tongue in E16.5 control (J,M), *Foxf1$^{c/c}$Foxf2$^{c/+}$Wnt1-Cre* (K,N) and *Foxf1$^{c/+}$Foxf2$^{c/c}$Wnt1-Cre* (L,O) embryos showing immunofluorescence detection of muscle actin (magenta) and collagen I (green). Panels M-O show higher-magnification views of the boxed areas in J-L, respectively. Arrows in M-O point to the location of the lingual septum tendon. Scale bars: 500 µm (A-C); 200 µm (D-L).

Examination of serial sections of the *Foxf1$^{c/+}$Foxf2$^{c/c}$Wnt1-Cre* mutant tongues also confirmed malformation of the Scx-GFP-positive lingual septum tendon and disorganization of the newly formed transverse muscle bundles (Fig. 4F,I). By E16.5, the lingual septum tendon was marked by high levels of collagen I in the middle of the tongue in control embryos (Fig. 4J,M). However, a collagen I-positive lingual septum tendon was not detected in either the *Foxf1$^{c/c}$Foxf2$^{c/+}$Wnt1-Cre* (Fig. 4K,N) or the *Foxf1$^{c/+}$Foxf2$^{c/c}$Wnt1-Cre* (Fig. 4L,O) mutant tongues, although a faint Scx-GFP+ lingual septum was detectable in the *Foxf1$^{c/+}$Foxf2$^{c/c}$Wnt1-Cre* embryos at this stage (Fig. 2C). These results indicate that Foxf1 and Foxf2 play crucial and partly redundant roles in lingual septum tendon formation.

Identification of Foxf2 target genes in tongue development

To uncover the molecular mechanism of how Foxf1/Foxf2 regulate tendon formation and myogenic cell differentiation during tongue development, we harvested tongue tissues from E12.5 *Foxf2$^{FLAG/FLAG}$* embryos, in which the endogenous Foxf2 protein contains a 3×FLAG epitope tag at the C-terminus (Xu et al., 2020), and performed chromatin immunoprecipitation sequencing (ChIP-seq) analysis using a well-characterized anti-FLAG antibody. We identified 25,707 high-quality Foxf2-associated peaks in the genome of E12.5 tongue tissues. The most enriched Foxf2-binding motif contained a core sequence, TGTTTAT/C (P=1×10^{-8973}, found at 61.05% target sites; Fig. 5A), which matched the Foxf1/Foxf2-binding motif identified previously from *in vivo* ChIP-seq using developing palatal tissues (Xu et al., 2020) and *in vitro* DNA-binding selection experiments (Hellqvist et al., 1996; Peterson et al., 1997). Gene Ontology (GO) analysis showed that Foxf2-binding sites were enriched in or near genes associated with ‘mesenchyme development’, ‘limb development’ and ‘palate development’ in the GO ‘biological process’ category (Fig. 5B). Interestingly, in the GO ‘molecular function’ category, Foxf2-binding sites were enriched in or near genes associated with the TGFβ signaling pathway (Fig. 5C). In particular, Foxf2 directly bound to the promoter regions of both *Tgfb2* and *Tgfb3* genes in the developing tongue (Fig. 5D,E). Furthermore, the Foxf2-binding peaks in the promoter region of both genes contained the Foxf1/Foxf2 binding motif (Fig. 5D,E), suggesting that the *Tgfb2* and *Tgfb3* genes are

Development (2022) 149, dev200667. doi:10.1242/dev.200667

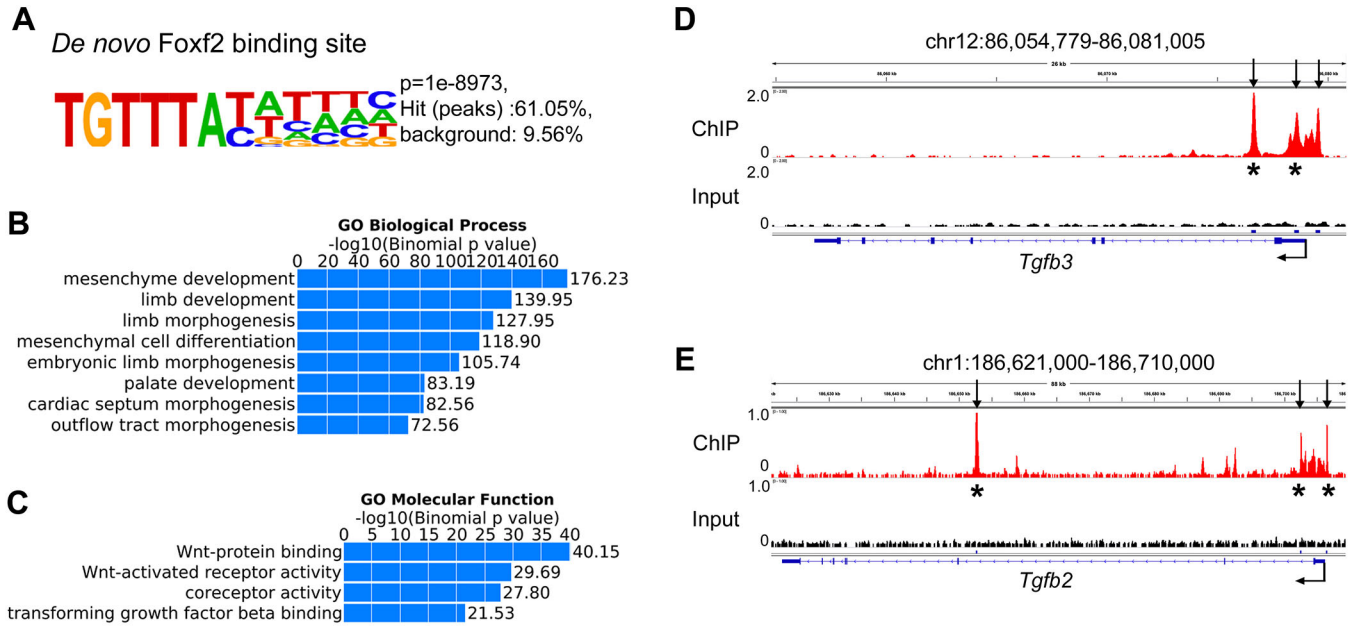

Fig. 5. Foxf2 directly binds to the promoter regions of the *Tgfb3* and *Tgfb2* genes in the developing tongue. (A) The sequence of the most enriched Foxf2-binding motif identified by ChIP-seq analysis of the E12.5 embryonic tongue is shown together with the statistical *P*-value and percentage of the ChIP-seq peaks containing the motif. (B,C) Gene Ontology analysis of the Foxf2 ChIP-seq peaks performed with GREAT (http://great.stanford.edu). The plot indicates the $-\log_{10}$ of binomial *P*-values of each GO term. The most significant GO biological process categories are shown in B and the most significant GO molecular function terms are shown in C. (D,E) Genome Browser views of the genomic regions containing the *Tgfb3* (D) and *Tgfb2* (E) genes. Vertical arrows point to the Foxf2-bound peak regions. Asterisks mark the ChIP-seq peaks containing the canonical Foxf1/Foxf2-binding motif.

direct downstream targets of Foxf1 and Foxf2 in tongue development.

Foxf1 and Foxf2 control the formation of the lingual septum tendon by regulating the TGFβ signaling pathway during tongue development

Previous studies have shown that TGFβ signaling plays a crucial role in tendon development. Disruption of TGFβ signaling in *Tgfb2*$^{-/-}$*Tgfb3*$^{-/-}$ embryos or through inactivation of the *Tgfbr2* gene resulted in the loss of most tendons and ligaments in mice (Pryce et al., 2009). We found that the expression of *Tgfb3* mRNA was enriched in the tendon progenitor cells in the tongue mesenchyme in E12.5 control embryos (Fig. 6A). In contrast, the expression of *Tgfb3* mRNA was undetectable by section *in situ* hybridization in the E12.5 *Foxf1*$^{c/c}$*Foxf2*$^{c/+}$*Wnt1-Cre* mutant tongue (Fig. 6B), and was also reduced in the E12.5 *Foxf1*$^{c/+}$*Foxf2*$^{c/c}$*Wnt1-Cre* mutant tongue (Fig. 6C). *Tgfb2* mRNA was broadly expressed at low levels in the tongue mesenchyme with no specific pattern of enrichment in the CNCC-derived mesenchyme in the control embryonic tongue at E12.5, but it was specifically reduced in the CNCC-derived mesenchyme in the *Foxf1*$^{c/c}$*Foxf2*$^{c/+}$*Wnt1-Cre* mutant tongue (Fig. 6D,E). *Tgfb2* mRNA expression was still detected in both the CNCC-derived mesenchyme and myogenic progenitor cells in the E12.5 *Foxf1*$^{c/+}$*Foxf2*$^{c/c}$*Wnt1-Cre* mutant tongue (Fig. 6F).

We next investigated whether the activity of the TGFβ signaling pathway was affected in the tongue mesenchyme in the *Foxf1*$^{c/c}$*Foxf2*$^{c/+}$*Wnt1-Cre* and *Foxf1*$^{c/+}$*Foxf2*$^{c/c}$*Wnt1-Cre* embryos. Immunofluorescence detection showed that phosphorylated Smad2 (pSmad2) was enriched in myogenic cells co-stained with muscle actin (Fig. 6G,J,M) and in the Scx-GFP+ tendon progenitor cells in the lingual septum (Fig. 6P,S) in E12.5 control embryos. In contrast, the *Foxf1*$^{c/c}$*Foxf2*$^{c/+}$*Wnt1Cre* embryonic tongue completely lacked the intense pSmad2-positive domains associated with the intrinsic muscles and midline lingual septum (Fig. 6H,K,N,Q,T), whereas the *Foxf1*$^{c/+}$*Foxf2*$^{c/c}$*Wnt1-Cre* embryonic tongue also showed reduced pSmad2 immunostaining associated with the intrinsic muscles and lingual septum (Fig. 6I,L,O,R,U). We further performed quantitative western blotting analysis and confirmed that the levels of phosphorylated Smad2 and Smad3 (pSmad2/3) proteins were significantly reduced in the *Foxf1*$^{c/c}$*Foxf2*$^{c/+}$*Wnt1-Cre* mutant tongues compared with those in control littermates (Fig. 6V,W). The levels of pSmad2/3 proteins in the E12.5 *Foxf1*$^{c/+}$*Foxf2*$^{c/c}$*Wnt1-Cre* tongue tissues were also reduced compared with those in control littermates, but the reduction was not statistically significant in the bulk tissue lysate (Fig. 6V,X). These results suggest that Foxf1 and Foxf2 act partly redundantly to regulate lingual tendon formation and intrinsic tongue muscle morphogenesis by controlling the activity of the TGFβ signaling pathway.

Hedgehog signaling acts upstream of *Hgf* expression in the CNCC-derived mandibular mesenchyme to regulate myoblast migration into the tongue primordium

Our ChIP-seq analysis also revealed multiple Foxf2-binding peaks near the *Hgf* gene (Fig. 7A), which encodes a secreted growth factor that plays crucial roles in guiding myoblast migration into the developing limb buds and tongue (Bladt et al., 1995; Dietrich et al., 1999; Yang et al., 1996). Comparison of the Foxf2-binding peaks around the *Hgf* gene with previously reported assay for transposase-accessible chromatin using sequencing (ATAC-seq) data from E10.5 mouse mandibular arch tissues (Minoux et al., 2017) showed that at least three Foxf2-binding sites containing the canonical Foxf2-binding motif were located in the promoter or putative cis-regulatory elements of the *Hgf* gene (Fig. 7A). As tongue agenesis in the *Smo*$^{c/c}$*Hand2-Cre* mouse embryos was associated with the loss of expression of both Foxf1 and Foxf2 in the mandibular arch mesenchyme (Xu et al., 2019) and failure of migration of the tongue

Development (2022) 149, dev200667. doi:10.1242/dev.200667

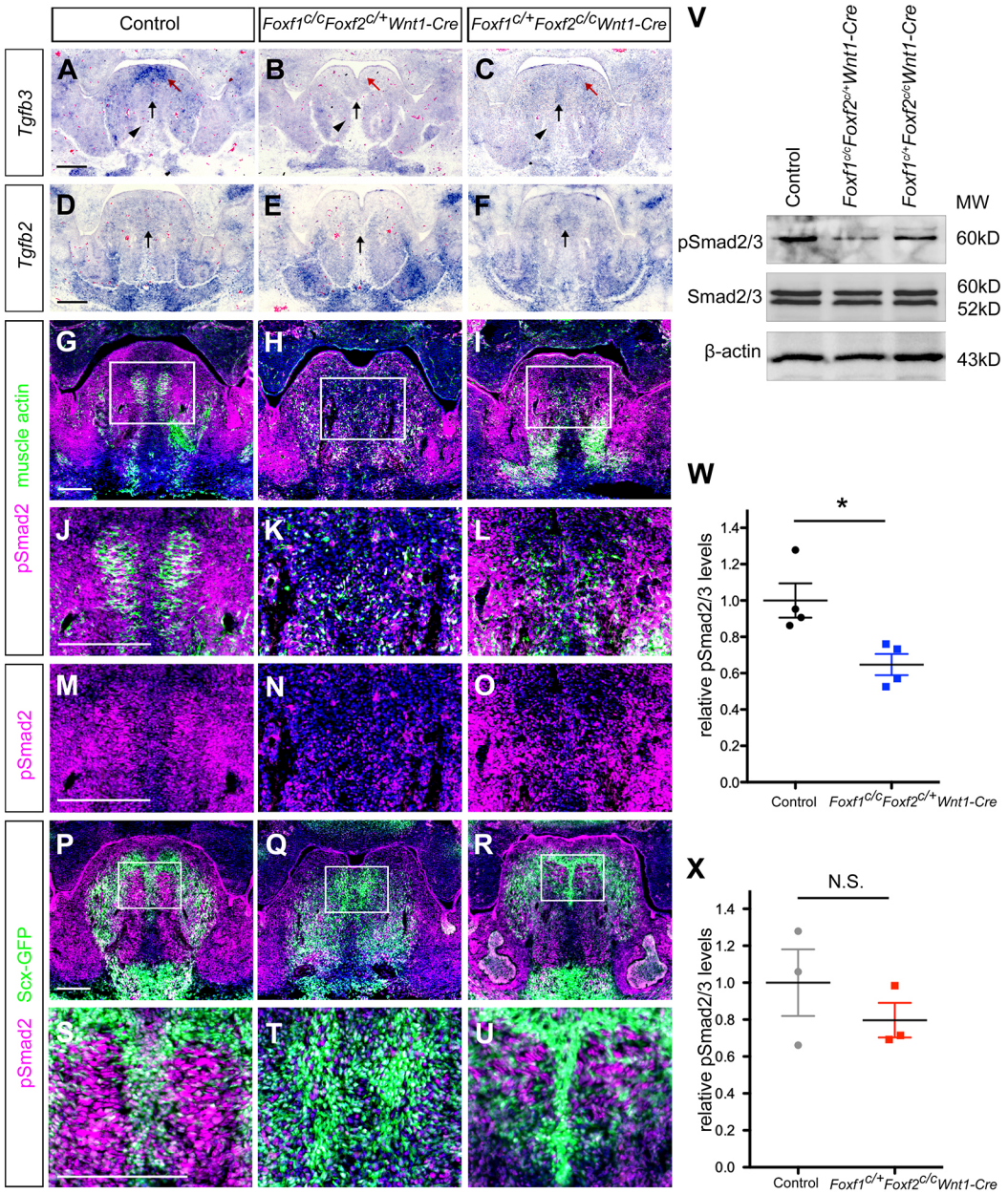

Fig. 6. Loss of Foxf1 and Foxf2 function in the CNCC-derived tongue mesenchyme affects TGFβ signaling in tongue development. (A-F) Frontal sections through the developing tongue in E12.5 control (A,D), *Foxf1*$^{c/c}$*Foxf2*$^{c/+}$*Wnt1-Cre* (B,E) and *Foxf1*$^{c/+}$*Foxf2*$^{c/c}$*Wnt1-Cre* (C,F) embryos showing patterns of expression of the *Tgfb3* (A-C) and *Tgfb2* (D-E) mRNAs (*n*=3 for each genotype). Black arrows point to the developing lingual septum. Red arrows point to the developing dorsal lingual aponeurosis. Black arrowheads point to the developing muscle. (G-O) Frontal sections through the developing tongue in E12.5 control (G,J,M), *Foxf1*$^{c/c}$*Foxf2*$^{c/+}$*Wnt1-Cre* (H,K,N) and *Foxf1*$^{c/+}$*Foxf2*$^{c/c}$*Wnt1-Cre* (I,L,O) embryos showing patterns of immunofluorescence staining of pSmad2 (magenta) and muscle actin (green) (*n*=3 for each genotype). Panels J-O show higher-magnification views of the boxed areas in G-I, respectively. (P-U) Frontal sections through the developing tongue in E12.5 control (P,S), *Foxf1*$^{c/c}$*Foxf2*$^{c/+}$*Wnt1-Cre* (Q,T) and *Foxf1*$^{c/+}$*Foxf2*$^{c/c}$*Wnt1-Cre* (R,U) embryos showing patterns of immunofluorescence staining of pSmad2 (magenta) and of the Scx-GFP reporter (green). Panels S-U show higher-magnification views of the boxed areas in P-R, respectively. (V) Western blot analysis of pSmad2/3, total Smad2/3 and β-actin in the E12.5 control, *Foxf1*$^{c/c}$*Foxf2*$^{c/+}$*Wnt1-Cre* and *Foxf1*$^{c/+}$*Foxf2*$^{c/c}$*Wnt1-Cre* tongue tissues. Images are representative of three embryos for each genotype. (W,X) Quantitative comparison of the levels of pSmad2/3 between the tongue tissues of control and *Foxf1*$^{c/c}$*Foxf2*$^{c/+}$*Wnt1-Cre* littermates (W) (*n*=4 for each genotype) and between control and *Foxf1*$^{c/+}$*Foxf2*$^{c/c}$*Wnt1-Cre* littermates (X) (*n*=3 for each genotype). Data are shown as mean±s.e.m. and compared by two-tailed unpaired *t*-test. N.S., not significant; *P<0.05. Scale bars: 200 µm.

muscle precursor cells into the mandibular arch (Fig. 7B,C), we investigated whether hedgehog signaling is required for HGF expression in the CNCC-derived mandibular mesenchyme for tongue myoblast migration. As previously reported, the *Hand2-Cre* transgenic mice express Cre specifically in the post-migratory CNCCs in the distal halves of the mandibular and other pharyngeal arches starting at E9.5 (Ruest et al., 2003; Xu et al., 2019). Genetic lineage tracing showed that the *Hand2-Cre* lineage contains all the CNCC-derived mandibular mesenchyme cells in the developing tongue anlage (Xu et al., 2019) (Fig. S4). Direct comparison of the patterns of expression of *Hgf* mRNA and the HGF protein with that of the *lacZ* reporter in the E11.5 *Hand2-Cre;R26R*^{lacZ} embryos

Development (2022) 149, dev200667. doi:10.1242/dev.200667

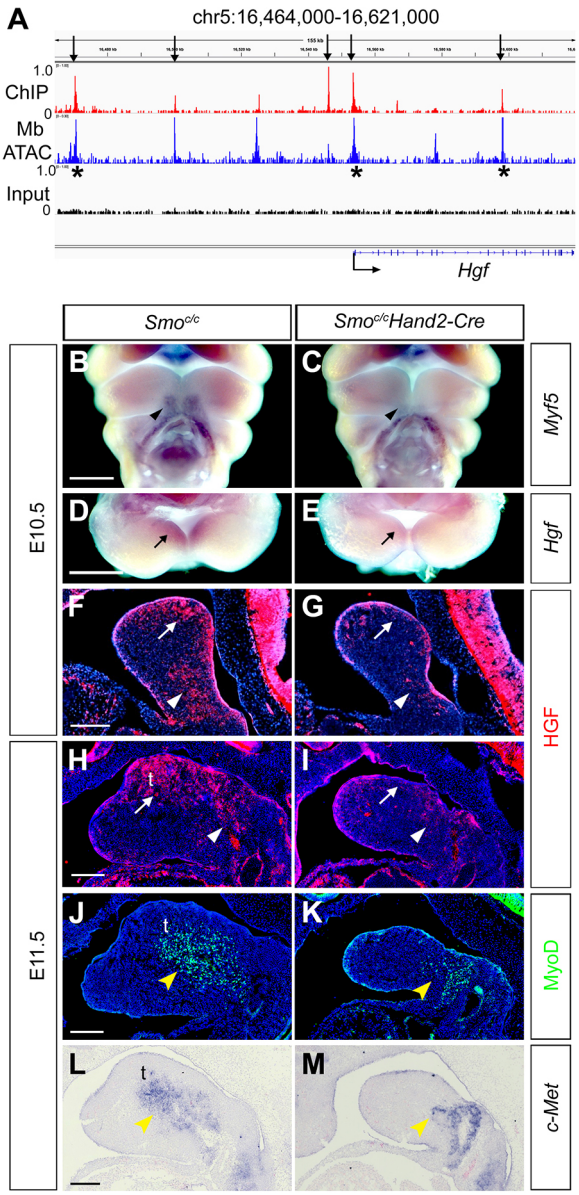

Fig. 7. Failure of myoblast migration into the developing tongue primordium in the *Smo$^{c/c}$Hand2-Cre* embryos correlated with loss of HGF expression in the mandibular arch. (A) Genome Browser view of the genomic region containing the *Hgf* gene. Vertical arrows point to the Foxf2-bound peak regions in E12.5 tongue tissues overlapping with the accessible chromatin regions in E10.5 mandibular tissues detected by ATAC-seq (Minoux et al., 2017). Asterisks mark the peaks containing the canonical Foxf1/Foxf2-binding motif. (B,C) Frontal views of E10.5 *Smo$^{c/c}$* control (B) and *Smo$^{c/c}$Hand2-Cre* (C) embryos showing failure of *Myf5*-expressing tongue myogenic progenitor cells to enter the mandibular arch in the *Smo$^{c/c}$Hand2-Cre* embryo in comparison with control littermates (*n*=3 for each genotype). Black arrowheads point to the *Myf5*-expressing tongue muscle precursor cells. (D,E) Rostral views of the mandibular arches showing patterns of *Hgf* mRNA expression in E10.5 *Smo$^{c/c}$* control (D) and *Smo$^{c/c}$Hand2-Cre* (E) embryos detected by whole-mount *in situ* hybridization. Black arrows point to the domain of *Hgf* mRNA expression in the oral side of the mandibular arch (*n*=3 for each genotype). (F-I) Sagittal sections through the developing mandibular arch of the *Smo$^{c/c}$* control (F,H) and *Smo$^{c/c}$Hand2-Cre* (G,I) embryos at E10.5 (F,G) and E11.5 (H,I), showing patterns of immunofluorescence staining of HGF (*n*=3 for each genotype at each stage). White arrows point to the domain of HGF expression in the tongue primordium and white arrowheads points to the domain of HGF expression in the caudal mandibular arch. (J,K) Sagittal sections through the mandibular arch of E11.5 *Smo$^{c/c}$* control (J) and *Smo$^{c/c}$Hand2-Cre* (K) embryos showing patterns of immunofluorescence staining of MyoD. Yellow arrowheads point to the MyoD-positive tongue muscle precursor cells. (L,M) Sagittal sections through the mandibular arch of E11.5 *Smo$^{c/c}$* control (L) and *Smo$^{c/c}$Hand2-Cre* (M) embryos showing patterns of *c-Met* mRNA expression (blue). Yellow arrowheads point to the domain of *c-Met* mRNA expression. t, tongue primordium. Scale bars: 500 µm (B-E); 200 µm (F-M).

showed that the *Hgf*-expressing cells in the tongue primordium were located within the *Hand2-Cre* lineage (Fig. S4E-G). Whereas highly restricted expression of *Hgf* mRNA and the HGF protein was detected in the oral domain of the developing mandibular arch in the *Smo$^{c/c}$* control embryos at E10.5 (Fig. 7D,F), expression of both *Hgf* mRNA and the HGF protein was dramatically reduced in the mandibular arch mesenchyme in the *Smo$^{c/c}$Hand2-Cre* littermates (Fig. 7E,G). At E11.5, the expression of HGF was enriched in the tongue primordium (Fig. 7H) in the *Smo$^{c/c}$* embryos, but was significantly reduced in the mandibular arch of *Smo$^{c/c}$Hand2-Cre* embryos (Fig. 7I). The HGF protein was also detected in the posterior region of the mandibular mesenchyme from E10.5 to E11.5 in control embryos, but was obviously reduced in the *Smo$^{c/c}$Hand2-Cre* mutant embryos (Fig. 7F-I). We examined the expression of *c-Met* (or *Met*), which encodes the cell surface receptor for HGF, in the tongue primordium. Consistent with previous reports (Amano et al., 2002), *c-Met* was expressed in the MyoD-positive myogenic progenitor cells (Fig. 7J,L). Although the myogenic progenitor cells migrated to the tongue primordium by E11.5 in the *Smo$^{c/c}$* embryos, few myoblasts migrated into the mandibular arch in the *Smo$^{c/c}$Hand2-Cre* littermates (Fig. 7J-M). Thus, the failure of tongue formation in the *Smo$^{c/c}$Hand2-Cre* embryos correlated with the loss of HGF expression in the CNCC-derived mandibular and tongue mesenchyme.

To further investigate the relationship between hedgehog signaling and HGF expression in tongue myogenesis, we crossed *Hand2-Cre* transgenic mice with the *R26SmoM2* mice, which carry a Cre-activatable transgene encoding a dominant active form of Smo (Jeong et al., 2004), and analyzed the expression of HGF in the mandibular mesenchyme in *R26SmoM2;Hand2-Cre* embryos. Whereas the E11.5 *R26SmoM2* embryos exhibited preferential localization of HGF in the tongue primordium, with MyoD-positive myoblasts migrating from the caudal distal region of the mandibular arch into the tongue primordium (Fig. S5A), the *R26SmoM2;Hand2-Cre* littermates exhibited high levels of HGF immunoreactivity in both the rostral and caudal domains of the developing mandibular arch with the MyoD-positive myoblasts scattered in the middle (Fig. S5B). Immunodetection of muscle actin on sagittal sections of the E16.5 *R26SmoM2;Hand2-Cre* embryonic heads showed a disorganized muscular structure in the mandible compared with the well-organized tongue musculature in control littermates (Fig. S5C,D). Remarkably, the caudal mandibular tissues, including the mandibular bone, were missing in the *R26SmoM2;Hand2-Cre* embryos (Fig. S5C,D). These results suggest that hedgehog signaling controls myoblast migration during tongue formation by regulating the expression of HGF in the CNCC-derived tongue mesenchyme.

Foxf1 and Foxf2 mediate the function of hedgehog signaling in regulating myoblast migration into the tongue primordium

The *Foxf1$^{c/c}$Foxf2$^{c/c}$Wnt1-Cre* mouse embryos displayed oral tongue agenesis (Fig. 8A,B), similarly as in the *Smo$^{c/c}$Hand2-Cre* mutant embryos (Xu et al., 2019). However, in contrast to the failure

Development (2022) 149, dev200667. doi:10.1242/dev.200667

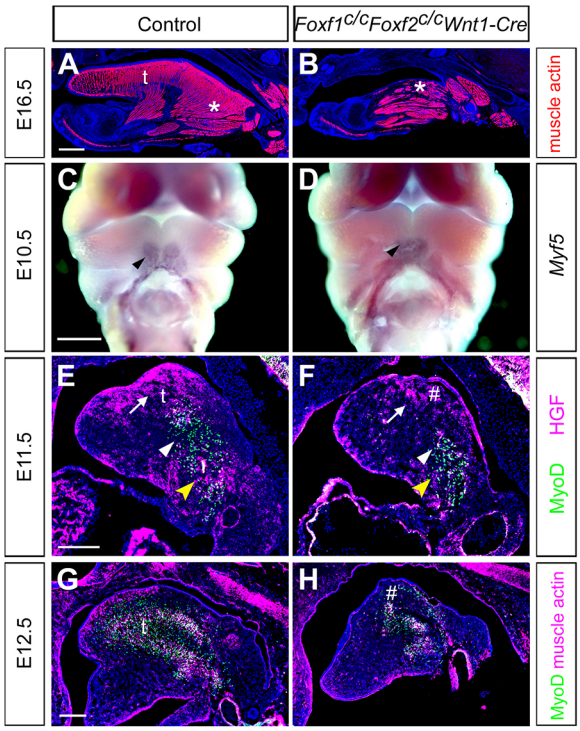

Fig. 8. Disruption of tongue myogenesis in the *Foxf1$^{c/c}$Foxf2$^{c/c}$Wnt1-Cre* embryos correlated with loss of HGF expression in the tongue primordium. (A,B) Sagittal sections through the tongue and mandible of E16.5 control (A) and *Foxf1$^{c/c}$Foxf2$^{c/c}$Wnt1-Cre* (B) embryos showing patterns of immunofluorescence staining of muscle actin (red). Asterisks mark the tongue muscle in the pharyngeal region. (C,D) Frontal views of E10.5 control (C) and *Foxf1$^{c/c}$Foxf2$^{c/c}$Wnt1-Cre* (D) embryos showing *Myf5*-expressing tongue muscle precursor cells migrating to the caudal mandibular arch (n=3 for each genotype). Black arrowheads point to the *Myf5*-positive (purple) tongue muscle precursor cells. (E,F) Sagittal sections through the developing tongue primordium of E11.5 control (E) and *Foxf1$^{c/c}$Foxf2$^{c/c}$Wnt1-Cre* (F) embryos showing patterns of immunofluorescence staining of HGF (magenta) and MyoD (green) (n=3 for each genotype). White arrows point to the expression of HGF in the tongue primordium. Yellow arrowheads point to the expression of HGF in the caudal mandibular arch. White arrowheads point to the MyoD-positive tongue muscle precursor cells. (G,H) Sagittal sections through the developing tongue of E12.5 control (G) and *Foxf1$^{c/c}$Foxf2$^{c/c}$Wnt1-Cre* (H) embryos showing patterns of immunofluorescence staining of muscle actin (magenta) and MyoD (green). The hash (#) indicates the agenesis of oral tongue tissue in *Foxf1$^{c/c}$Foxf2$^{c/c}$Wnt1-Cre* (F,H) embryos. t, tongue. Scale bars: 500 µm (A-D); 200 µm (E-H).

of migration of tongue muscle precursor cells from the hypoglossal cord into the mandibular arches in the *Smo$^{c/c}$Hand2-Cre* mutant embryos (Fig. 7B,C), the *Myf5*-expressing tongue myogenic precursor cells migrated into the caudal distal region of the mandibular arch in the *Foxf1$^{c/c}$Foxf2$^{c/c}$Wnt1Cre* embryos by E10.5, similarly as in control littermates (Fig. 8C,D). From E11.5 to E12.5, the MyoD-positive myogenic progenitor cells migrated into the tongue primordium and started to form muscle actin-positive myotubes in the *Foxf1$^{c/c}$Foxf2$^{c/c}$* control embryos (Fig. 8E,G), but MyoD-positive myogenic progenitor cells failed to migrate into the tongue primordium in the *Foxf1$^{c/c}$Foxf2$^{c/c}$Wnt1-Cre* mutant embryos (Fig. 8F,H). Immunofluorescence staining of the HGF protein showed that HGF was enriched in the tongue primordium and posterior region of the mandibular mesenchyme in *Foxf1$^{c/c}$Foxf2$^{c/c}$* control embryos, and was reduced in the tongue primordium in the *Foxf1$^{c/c}$Foxf2$^{c/c}$Wnt1-Cre* mutant embryos (Fig. 8E,F). Moderate levels of the HGF protein were detected surrounding the myoblasts in the posterior region of the mandibular arches in the *Foxf1$^{c/c}$Foxf2$^{c/c}$Wnt1Cre* mutant embryos (Fig. 8F). Furthermore, we found that the E11.5 *Foxf1$^{c/c}$Foxf2$^{c/+}$Wnt1-Cre* embryos had reduced HGF immunostaining compared with control littermates, particularly at the anterior region of the developing tongue primordium. This reduced staining correlated with the scattering of MyoD-positive myoblasts in the posterior mandibular arch in *Foxf1$^{c/c}$Foxf2$^{c/+}$Wnt1-Cre* embryos, compared with the concentrated myoblasts migrating toward the tongue primordium in control and *Foxf1$^{c/+}$Foxf2$^{c/c}$Wnt1Cre* littermates (Fig. S6A-C). Taken together, these results indicate that although Foxf1/Foxf2 are not essential for the initial migration of the tongue muscle precursor cells into the distal mandibular arch, Foxf1/Foxf2 act downstream of hedgehog signaling to regulate HGF expression in the CNCC-derived tongue mesenchyme to direct myoblast migration into the tongue primordium.

DISCUSSION

The molecular mechanisms controlling the development of the tongue are not well understood and remain understudied. In this report, we demonstrate that the Foxf1/Foxf2 transcription factors mediate crucial roles of hedgehog signaling in regulating multiple steps of tongue morphogenesis. During the initiation stage of tongue formation, hedgehog-Foxf1/Foxf2 signaling, by regulating the expression of HGF in the CNCC-derived tongue mesenchyme, directs the migration of c-Met+ myoblasts into the tongue primordium (Fig. 9A). After myoblast arrival in the tongue primordium, Foxf1/Foxf2 continue to be expressed in the CNCC-derived tongue mesenchyme and control lingual tendon formation and subsequently the differentiation and morphogenesis of intrinsic tongue muscles by regulating the activity of the TGFβ signaling pathway (Fig. 9B).

Hedgehog-Foxf1/Foxf2 signaling regulates HGF expression to direct the migration of myoblasts into the tongue primordium

In both *Smo$^{c/c}$Hand2-Cre* and *Foxf1$^{c/c}$Foxf2$^{c/c}$Wnt1-Cre* mutant embryos, myoblasts failed to migrate into the tongue primordium, resulting in oral tongue agenesis (Jeong et al., 2004; Xu et al., 2019; this study). Previous studies showed that HGF and its cognate receptor c-Met play a crucial role in regulating delamination and migration of myogenic progenitor cells to give rise to the tongue musculature, the muscular diaphragm, the limb and associated shoulder musculature (Bladt et al., 1995; Dietrich et al., 1999). During tongue development in mouse embryos, expression of the HGF protein was first detected in the oral side of the mandibular arch mesenchyme at E10, and both *Hgf* mRNA and the HGF protein continued to be expressed in the developing tongue mesenchyme through E15 (Amano et al., 2002). Using an explant culture system, previous studies showed that HGF plays important roles in the early tongue primordium by promoting both the migration and proliferation of myoblasts through c-Met in paracrine and autocrine manners (Amano et al., 2002; Yamane et al., 2003). However, the molecular mechanism regulating *Hgf* gene expression during tongue development remained unknown. We found that the expression of HGF was dramatically reduced in the mandibular arch of *Smo$^{c/c}$Hand2-Cre* embryos and in the tongue primordium of *Foxf1$^{c/c}$Foxf2$^{c/c}$Wnt1-Cre* mutant embryos (Figs 7 and 8), and that HGF expression was expanded in the mandibular mesenchyme of the *R26SmoM2;Hand2-Cre* embryos (Fig. S5). Our ChIP-seq analysis showed that Foxf2 directly bound to the promoter and

Development (2022) 149, dev200667. doi:10.1242/dev.200667

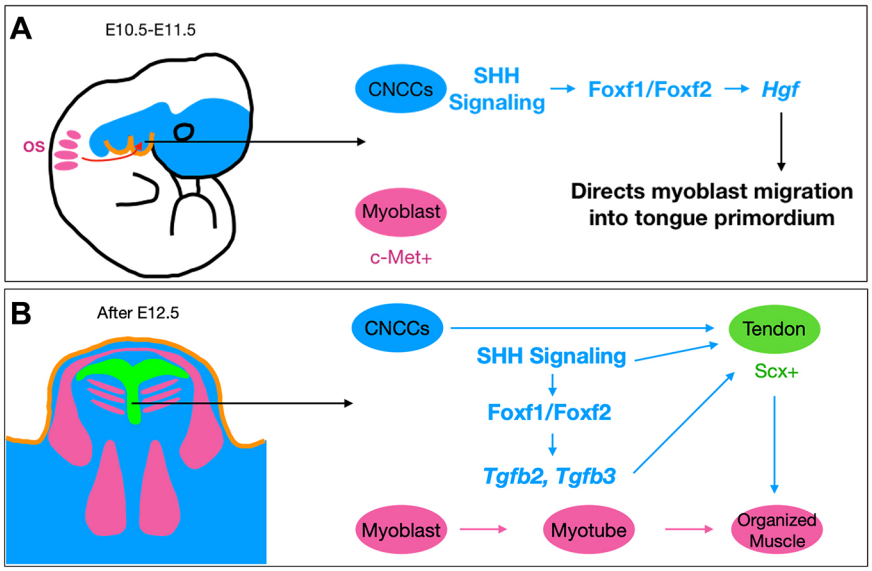

Fig. 9. The roles of hedgehog-Foxf1/Foxf2 signaling in tongue morphogenesis. (A) At the initiation stage of tongue myogenesis, SHH-Foxf1/Foxf2 signaling regulates the expression of HGF in the CNCC-derived mandibular mesenchyme to direct the migration of c-Met+ myoblasts into the tongue primordium. (B) After myoblast arrival in the tongue primordium, Foxf1/Foxf2 in the CNCC-derived tongue mesenchyme control lingual tendon formation and subsequently the morphogenesis of intrinsic tongue muscles by regulating the expression *Tgfb2* and *Tgfb3*. The CNCC-derived mesenchyme is indicated in blue, myogenic cells are indicated in magenta, Scx+ tendon progenitors in fibrous lingual septum at the midline and the dorsal submucosal lingual aponeurosis are indicated in green. os, occipital somites.

putative enhancer regions of the *Hgf* gene in the tongue primordium, suggesting that hedgehog-Foxf1/Foxf2 signaling directly regulates the transcriptional activation of *Hgf* gene expression to control tongue formation.

Distinct from the complete failure of migration of tongue myoblasts into the mandibular arches in the *Smo$^{c/c}$Hand2-Cre* embryos, the tongue myoblasts were able to migrate into the mandibular arches but failed to further migrate into the tongue primordium in the *Foxf1$^{c/c}$Foxf2$^{c/c}$Wnt1-Cre* embryos (Fig. 8) (Xu et al., 2019). High levels of HGF expression were detected in the prospective tongue mesenchyme as well as in the posterior region of the mandibular mesenchyme from E10.5 to E11.5 in control embryos, but HGF expression was dramatically reduced in both domains in the *Smo$^{c/c}$Hand2-Cre* mutant embryos (Fig. 7F,G). In the *Foxf1$^{c/c}$Foxf2$^{c/c}$Wnt1-Cre* embryos, HGF expression was also reduced in both mandibular domains in comparison with control littermates, but mesenchymal cells expressing moderate levels of HGF surrounded the myoblasts in the caudal proximal region of the mandibular arches in the *Foxf1$^{c/c}$Foxf2$^{c/c}$Wnt1Cre* mutant embryos (Fig. 8E,F). Several other Forkhead genes, including *Foxd1* and *Foxd2*, are expressed in the developing mandibular arches in partly overlapping patterns with those of *Foxf1* and *Foxf2*, and expression of both *Foxd1* and *Foxd2* in the mandibular arch mesenchyme also depend on hedgehog signaling (Jeong et al., 2004). It is possible that the other Forkhead genes partly complemented Foxf1/Foxf2 function in the regulation of *Hgf* gene expression in the mandibular mesenchyme, and that in the *Foxf1$^{c/c}$Foxf2$^{c/c}$Wnt1-Cre* embryos, the moderate levels of HGF expression was sufficient to guide the tongue myoblasts into the caudal region of the mandibular arch, but was insufficient for directing the myoblasts into the tongue primordium. Further studies are needed to uncover other factors that partly complemented Foxf1/Foxf2 function downstream of hedgehog signaling in the regulation of HGF expression and tongue myoblast migration.

We previously showed that the SHH-Foxf1/Foxf2 pathway regulates oral-aboral patterning of the mandibular arch by antagonizing BMP signaling (Xu et al., 2019). *Shh* and *Bmp4* exhibit complementary patterns of expression in the distal mandibular arch epithelium and their target genes are expressed in a complementary pattern along the oral-aboral axis in the early mandibular arch mesenchyme (Xu et al., 2019). Both *Smo$^{c/c}$Hand2-Cre* and *Foxf1$^{c/c}$Foxf2$^{c/c}$Wnt1-Cre* embryos exhibited dramatic expansion of BMP signaling activity and target gene expression throughout the oral side of the distal mandibular arch and, subsequently, duplication of the mandibular bone at the oral side at the expense of tongue formation (Xu et al., 2019). We found that the *Foxf1$^{c/c}$Foxf2$^{c/+}$Wnt1-Cre* embryos, but not the *Foxf1$^{c/+}$Foxf2$^{c/c}$Wnt1-Cre* embryos, exhibited expanded expression of the BMP target genes *Msx1* and *Msx2* to the oral side at the most distal region of the mandibular arches at E10.5. Whereas no overt disruption of the oral-aboral axis of mandibular structures was observed in the *Foxf1$^{c/c}$Foxf2$^{c/+}$Wnt1-Cre* embryos at later developmental stages, the tongue in the *Foxf1$^{c/c}$Foxf2$^{c/+}$Wnt1-Cre* embryos was significantly smaller than that in control littermates. It has been reported previously that BMP signaling restricts the position of premuscle masses in the developing limb buds by indirectly antagonizing HGF-directed myoblast migration to the anterior, posterior and distal limb bud margins (Bonafede et al., 2006). We found that the *Foxf1$^{c/c}$Foxf2$^{c/+}$Wnt1-Cre* embryos exhibited aberrant scattering of myoblasts in the posterior region of the mandibular arch at E11.5 and a significantly reduced proportion of myoblasts in the anterior half with a concomitant significant increase in the proportion of myoblasts in the posterior half of the developing tongue by E12.5. It is possible that the orally expanded BMP signaling activity in the distal mandibular arch contributed to the impairment of myoblast migration into the tongue primordium and the subsequent anteriorward outgrowth of the tongue in the *Foxf1$^{c/c}$Foxf2$^{c/+}$Wnt1-Cre* embryos. Thus, both Foxf1/Foxf2-mediated suppression of BMP signaling activity in the oral side of the mandibular arch mesenchyme and Foxf1/Foxf2-mediated activation of HGF expression are important for the directional migration of the tongue muscle precursor cells into the tongue primordium.

Foxf1/Foxf2 mediates hedgehog signaling regulation of lingual tendon formation and intrinsic tongue muscle morphogenesis through regulation of TGFβ signaling

Tendons are connective tissues anchoring muscles to bones and transmit forces generated by muscle to bone, which confer the integrity and mobility of the musculoskeletal system. Previous studies have shown that hedgehog signaling plays important roles in tendon development, including lingual tendon formation (Liu et al.,

Development (2022) 149, dev200667. doi:10.1242/dev.200667

2012, 2013; Okuhara et al., 2019; Schwartz et al., 2015). Okuhara et al. (2019) showed that the $Shh^{MFCS4/-}$ mouse embryos exhibited significantly reduced expression of *Scx* and *Col1a1* mRNAs in the developing tongue (Okuhara et al., 2019). They showed that the expression of both *Tgfb2* and *Tgfb3* was reduced in the intrinsic tongue musculature in $Shh^{MFCS4/-}$ embryos by *in situ* hybridization analysis and that induced global inactivation of *Shh* at E10.5 caused reduction in the amount of pSmad2/3 in the developing tongue at E14.5 by western blot analysis (Okuhara et al., 2019). However, these results could not distinguish whether SHH signaling directly or indirectly regulates the organization of the tongue musculature and how SHH signaling regulates TGFβ signaling during tongue development. Here, we showed that in the $Foxf1^{c/c}Foxf2^{c/+}$*Wnt1-Cre* and $Foxf1^{c/+}Foxf2^{c/c}$*Wnt1-Cre* mutant embryos, the formation of the lingual septum tendon was disrupted, leading to an absence or disorganization of specific intrinsic muscles of the tongue. The activity of TGFβ signaling was downregulated in the developing tongue in the $Foxf1^{c/c}Foxf2^{c/+}$*Wnt1-Cre* and $Foxf1^{c/+}Foxf2^{c/c}$*Wnt1-Cre* mutant embryos. As Foxf1 and Foxf2 have been shown to be important mediators of hedgehog signaling during multiple craniofacial developmental processes (Jeong et al., 2004; Lan and Jiang, 2009; Xu et al., 2019), these results indicate that Foxf1 and Foxf2 act downstream of hedgehog signaling in the CNCC-derived tongue mesenchyme to regulate the formation of the lingual septum tendon.

Our ChIP-seq analysis showed that Foxf2-binding peaks in the developing tongue cells were enriched near the genes associated with the TGFβ signaling pathway. Foxf2 occupied the promoter regions of the *Tgfb2* and *Tgfb3* genes in the developing tongue. It has been shown that inactivation of *Tgfbr2* in CNCCs (*Wnt1-Cre;*$Tgfbr2^{flox/flox}$) resulted in microglossia with reduced *Scx* expression, decreased myogenic cell proliferation and disorganized tongue muscles (Hosokawa et al., 2010). Inactivation of *Tgfbr1* (*Alk5*) in CNCCs (*Wnt1-Cre;*$Alk5^{fl/fl}$) also caused severely disrupted tongue muscles with reduced myogenic cell proliferation and differentiation (Han et al., 2014). TGFβ signaling also plays a crucial role in the formation of tendons and ligaments. Loss of TGFβ signaling in $Tgfb2^{-/-}$;$Tgfb3^{-/-}$ embryos or through inactivation of the type II TGFβ receptor resulted in the agenesis of most tendons and ligaments in the limbs, trunk, tail and head (Pryce et al., 2009). We found that *Tgfb2* and *Tgfb3* exhibited different patterns of expression in the developing tongue, with *Tgfb3* expression enriched in the central and dorsal regions of the tongue mesenchyme, whereas *Tgfb2* mRNAs were expressed at low levels in both the neural crest-derived and myogenic tongue mesenchyme, indicating that their patterns of expression in the developing tongue are differentially regulated and may involve Foxf1/Foxf2 and other transcription factors. We found that the expression of *Tgfb3* was dramatically downregulated in the tendon progenitor cells in both $Foxf1^{c/c}Foxf2^{c/+}$*Wnt1-Cre* and $Foxf1^{c/+}Foxf2^{c/c}$*Wnt1-Cre* mutant tongue, whereas the expression of *Tgfb2* was also reduced in the CNCC-derived mesenchyme in the $Foxf1^{c/c}Foxf2^{c/+}$*Wnt1-Cre* mutant tongue. Furthermore, we found that the $Foxf1^{c/c}Foxf2^{c/+}$*Wnt1-Cre* and $Foxf1^{c/+}Foxf2^{c/c}$*Wnt1-Cre* embryos exhibited reduced pSmad2 in the progenitor cells of the lingual septum tendon as well as in the neighboring intrinsic tongue muscle progenitor cells. Taken together, these results indicate that the Foxf1/Foxf2 transcription factors regulate lingual tendon formation and tongue muscle morphogenesis at least in part by controlling the expression of *Tgfb2* and *Tgfb3* in the CNCC-derived tongue mesenchyme.

MATERIALS AND METHODS

Mice

The $Smo^{c/c}$, *R26SmoM2*, $Foxf1^{c/c}$, $Foxf2^{c/c}$, *Wnt1-Cre*, *Hand2-Cre*, *Scx-GFP*, $R26R^{lacZ}$, $R26R^{mTmG}$ and $Foxf2^{FLAG}$ mice have been described previously (Bolte et al., 2015; Danielian et al., 1998; Jeong et al., 2004; Long et al., 2001; Muzumdar et al., 2007; Pryce et al., 2007; Ren et al., 2014; Ruest et al., 2003; Soriano, 1999; Xu et al., 2020). The *Hand2-Cre* and *Wnt1-Cre* mice were maintained by crossing with CD1 (Charles River) mice. $Smo^{c/c}$, *R26SmoM2*, $Foxf1^{c/c}$, $Foxf1^{c/c}$;*Scx-GFP*, $Foxf2^{c/c}$, $Foxf2^{c/c}$;*Scx-GFP*, $R26R^{LacZ}$, $R26R^{mTmG}$ and $Foxf2^{FLAG}$ mice were maintained by intercrossing. E0.5 was designated as the noon of the day on which a vaginal plug was identified. *Cre*-negative littermates were used as control samples in experiments. Both female and male embryos were used in this study. The stages of the embryos are indicated in the main text and figure legends. This study was performed in strict accordance with the recommendations in the Guide for the Care and Use of Laboratory Animals by the National Institutes of Health. The animal use protocol was approved by the Institutional Animal Care and Use Committee of Cincinnati Children's Hospital Medical Center (Protocol number IACUC2019-0073).

In situ hybridization, skeletal preparations and mandibular bone length measurement

For *in situ* hybridization analysis of paraffin sections, embryos were dissected at the desired stages from timed pregnant mice, fixed in 4% paraformaldehyde, dehydrated through an ethanol series, embedded in paraffin and sectioned at 7 µm thickness using a Leica RM2125 microtome. Whole-mount and section *in situ* hybridization were performed as previously described (Lan et al., 2001; Zhang et al., 1999).

Skeletal preparations of P0 embryos were processed and stained with Alizarin Red and Alcian Blue as previously described (Martin et al., 1995). Quantitative comparison of the length of the mandibular bone was performed by measuring the length from the distal tip of the mandibular bone to the end of the condylar process using NIS-Elements AR software (version 5.41.01, Nikon). The results are presented as mean±s.e.m. Statistical analysis was performed by using two-tailed unpaired Student's *t*-test using GraphPad Prism. $P<0.05$ was considered statistically significant.

Immunofluorescence staining and quantification of myoblast distribution

Immunofluorescence staining of paraffin sections was performed following standard protocols (Xu et al., 2014). The following primary antibodies were used: rabbit anti-Sox9 (Abcam, ab185230, 1:200), rabbit anti-MyoD (Abcam, ab133627, 1:100) and rabbit anti-Collagen I (Abcam, ab34710, 1:100). The anti-muscle actin antibody (Clone HUC1-1, 1:1000) (Sawtell and Lessard, 1989) was provided by Dr James Lessard (Cincinnati Children's Hospital Medical Center). Immunofluorescence staining on frozen sections was performed as described previously (Xu et al., 2019). The following primary antibodies were used: sheep anti-Foxf2 (R&D Systems, AF6988, 1:50), goat anti-Foxf1 (R&D Systems, AF4798, 1:50), goat anti-HGF (R&D Systems, AF-294, 1:50), rabbit anti-MyoD (Abcam, ab133627, 1:100), anti-muscle actin (Clone HUC1-1, 1:1000) (Sawtell and Lessard, 1989), rabbit anti-β-galactosidase (Invitrogen, A-11132, 1:200) and rabbit anti-pSmad2 (Cell Signaling Technology, 3108, 1:50). Images were taken using a Nikon DS-Qi2 microscope (Nikon Instruments).

To quantify MyoD+ myoblast distribution in the developing tongue, whole heads from $Foxf1^{c/c}Foxf2^{c/+}$*Wnt1-Cre*, $Foxf1^{c/+}Foxf2^{c/c}$*Wnt1-Cre* and control embryos at E12.5 were dissected. Serial coronal sections were collected and the sections containing the tongue tissues were divided into posterior and anterior regions. In each section, the developing tongue tissues were divided into medial and lateral domains (Fig. 3G). MyoD+ myoblasts and DAPI+ nuclei were counted using NIS-Elements AR software. The percentage of MyoD+ cells was calculated using the number of MyoD+ nuclei divided by the number of total nuclei. The results are presented as mean±s.d. Statistical analysis was performed by using two-tailed unpaired Student's *t*-test. $P<0.05$ was considered statistically significant.

Development (2022) 149, dev200667. doi:10.1242/dev.200667

Western blot analysis

Whole tongue tissues were dissected from *Foxf1*$^{c/c}$*Foxf2*$^{c/+}$*Wnt1-Cre*, *Foxf1*$^{c/+}$*Foxf2*$^{c/c}$*Wnt1-Cre* and control (Cre-negative littermates) embryos at E12.5. Two tongues of the same genotype were pooled into one sample and lysed in radioimmunoprecipitation assay (RIPA) buffer (Santa Cruz Biotechnology, sc-24948). Equivalent amounts of protein lysate were subjected to SDS-PAGE and transferred to polyvinylidene difluoride membranes (Bio-Rad, 1620177). The following antibodies were used: rabbit anti-pSmad2/3 (Cell Signaling Technology, 8828, 1:500), rabbit anti-Smad2/3 (Cell Signaling Technology, 8685, 1:1000) and mouse anti-β-actin (Santa Cruz Biotechnology, sc-47778 HRP, 1:10,000). Images were taken using ChemiDoc MP Imaging System (Bio-Rad). The intensities of detected bands on western blots were quantified using Photoshop Histogram Analysis. pSmad2/3 band intensities were normalized against total Smad2/3 band intensities. The results are presented as mean±s.e.m. Statistical analysis was performed by using two-tailed unpaired Student's *t*-test using GraphPad Prism. $P<0.05$ was considered statistically significant.

ChIP-seq and data analysis

Tongue tissues were manually dissected from 75 E12.5 *Foxf2*$^{FLAG/FLAG}$ embryos and processed for ChIP as previously described (Park et al., 2012; Xu et al., 2020). Briefly, tissues were crosslinked with 1% paraformaldehyde. Following sonication and extraction of DNA/protein complexes, samples were incubated with anti-FLAG antibody (Sigma-Aldrich, F1804). Sequencing libraries were generated using the ThruPLEX DNA sequencing kit (Takara). Sequencing was performed on an Illumina Nextseq 500 sequencer. For ChIP-seq data analysis, raw FASTQ files were aligned to the mm10 reference mouse genome using Bowtie2 (2.4.1). Peak calling and *de novo* motif identification were performed using the Hypergeometric Optimization of Motif EnRichment (HOMER) software (version 4.11.1). To identify reproducible Foxf2-binding peaks, we performed two steps of differential analysis comparing ChIP versus input samples. Initially, Foxf2-FLAG peaks from two biological replicates were pooled and merged to generate a preliminary peak set with default settings, which required at least fourfold enrichment over input. Peaks were further filtered by a peak score above 10. The read counts were measured in each individual ChIP and input samples within the peak set. Differential expression analysis was performed using DEseq2 (Love et al., 2014). Final peaks were defined by a false discovery rate of less than 0.01. Region-gene association and GO analysis were performed using the online Genomic Regions Enrichment of Annotations Tool (GREAT) program, version 4.0.4 (http://great.stanford.edu). The 'basal plus extension' parameter was used to associate genomic regions to genes. The ChIP-seq data from this study have been deposited into the National Center for Biotechnology Information Gene Expression Omnibus (GEO) database (accession number GSE195788). ATAC-seq data and the processed wig file of E10.5 mandible were obtained from GEO (dataset GSE89436) (Minoux et al., 2017).

Acknowledgements

We thank the Cincinnati Children's Hospital Medical Center DNA Sequencing and Genotyping core facility for their DNA sequencing service.

Competing interests

The authors declare no competing or financial interests.

Author contributions

Conceptualization: J.X., R.J.; Methodology: J.X., H.L.; Validation: J.X.; Formal analysis: J.X., H.L., Y.L., R.J.; Investigation: J.X., H.L., Y.L., R.J.; Resources: R.J.; Data curation: J.X., H.L.; Writing - original draft: J.X.; Writing - review & editing: J.X., H.L., Y.L., R.J.; Visualization: J.X., H.L., Y.L., R.J.; Supervision: Y.L., R.J.; Project administration: Y.L., R.J.; Funding acquisition: R.J.

Funding

This work was supported by the National Institutes of Health/National Institute of Dental and Craniofacial Research (NIH/NIDCR) grants DE027046 and DE029417. The content is solely the responsibility of the authors and does not necessarily represent the official views of the National Institutes of Health. Deposited in PMC for release after 12 months.

Data availability

ChIP-seq data have been deposited into the Gene Expression Omnibus with the accession number GSE195788.

Peer review history

The peer review history is available online at https://dev.biologists.org/lookup/doi/10.1242/dev.200667.reviewer-comments.pdf.

References

Amano, O., Yamane, A., Shimada, M., Koshimizu, U., Nakamura, T. and Iseki, S. (2002). Hepatocyte growth factor is essential for migration of myogenic cells and promotes their proliferation during the early periods of tongue morphogenesis in mouse embryos. *Dev. Dyn.* **223**, 169-179. doi:10.1002/dvdy.1228

Billmyre, K. K. and Klingensmith, J. (2015). Sonic hedgehog from pharyngeal arch 1 epithelium is necessary for early mandibular arch cell survival and later cartilage condensation differentiation. *Dev. Dyn.* **244**, 564-576. doi:10.1002/dvdy.24256

Bladt, F., Riethmacher, D., Isenmann, S., Aguzzi, A. and Birchmeier, C. (1995). Essential role for the c-met receptor in the migration of myogenic precursor cells into the limb bud. *Nature* **376**, 768-771. doi:10.1038/376768a0

Bolte, C., Ren, X., Tomley, T., Ustiyan, V., Pradhan, A., Hoggatt, A., Kalin, T. V., Herring, B. P. and Kalinichenko, V. V. (2015). Forkhead box F2 regulation of platelet-derived growth factor and myocardin/serum response factor signaling is essential for intestinal development. *J. Biol. Chem.* **290**, 7563-7575. doi:10.1074/jbc.M114.609487

Bonafede, A., Köhler, T., Rodriguez-Niedenführ, M. and Brand-Saberi, B. (2006). BMPs restrict the position of premuscle masses in the limb buds by influencing Tcf4 expression. *Dev. Biol.* **299**, 330-344. doi:10.1016/j.ydbio.2006.02.054

Briscoe, J. (2009). Making a grade: Sonic Hedgehog signalling and the control of neural cell fate. *EMBO J.* **28**, 457-465. doi:10.1038/emboj.2009.12

Briscoe, J. and Vincent, J.-P. (2013). Hedgehog threads to spread. *Nat. Cell Biol.* **15**, 1265-1267. doi:10.1038/ncb2878

Brito, J. M., Teillet, M.-A. and Le Douarin, N. M. (2006). An early role for sonic hedgehog from foregut endoderm in jaw development: ensuring neural crest cell survival. *Proc. Natl. Acad. Sci. USA* **103**, 11607-11612. doi:10.1073/pnas.0604751103

Clark, K. L., Halay, E. D., Lai, E. and Burley, S. K. (1993). Co-crystal structure of the HNF-3/fork head DNA-recognition motif resembles histone H5. *Nature* **364**, 412-420. doi:10.1038/364412a0

Cobourne, M. T., Iseki, S., Birjandi, A. A., Adel Al-Lami, H., Thauvin-Robinet, C., Xavier, G. M. and Liu, K. J. (2019). How to make a tongue: cellular and molecular regulation of muscle and connective tissue formation during mammalian tongue development. *Semin. Cell Dev. Biol.* **91**, 45-54. doi:10.1016/j.semcdb.2018.04.016

Danielian, P. S., Muccino, D., Rowitch, D. H., Michael, S. K. and McMahon, A. P. (1998). Modification of gene activity in mouse embryos in utero by a tamoxifen-inducible form of Cre recombinase. *Curr. Biol.* **8**, 1323-1326. doi:10.1016/S0960-9822(07)00562-3

Dietrich, S., Abou-Rebyeh, F., Brohmann, H., Bladt, F., Sonnenberg-Riethmacher, E., Yamaai, T., Lumsden, A., Brand-Saberi, B. and Birchmeier, C. (1999). The role of SF/HGF and c-Met in the development of skeletal muscle. *Development* **126**, 1621-1629. doi:10.1242/dev.126.8.1621

Ericson, J., Briscoe, J., Rashbass, P., van Heyningen, V. and Jessell, T. M. (1997). Graded sonic hedgehog signaling and the specification of cell fate in the ventral neural tube. *Cold Spring Harb. Symp. Quant. Biol.* **62**, 451-466. doi:10.1101/SQB.1997.062.01.053

Han, A., Zhao, H., Li, J., Pelikan, R. and Chai, Y. (2014). ALK5-mediated transforming growth factor β signaling in neural crest cells controls craniofacial muscle development via tissue-tissue interactions. *Mol. Cell. Biol.* **34**, 3120-3131. doi:10.1128/MCB.00623-14

Haworth, K. E., Wilson, J. M., Grevellec, A., Cobourne, M. T., Healy, C., Helms, J. A., Sharpe, P. T. and Tucker, A. S. (2007). Sonic hedgehog in the pharyngeal endoderm controls arch pattern via regulation of Fgf8 in head ectoderm. *Dev. Biol.* **303**, 244-258. doi:10.1016/j.ydbio.2006.11.009

Hellqvist, M., Mahlapuu, M., Samuelsson, L., Enerbäck, S. and Carlsson, P. (1996). Differential activation of lung-specific genes by two forkhead proteins, FREAC-1 and FREAC-2. *J. Biol. Chem.* **271**, 4482-4490. doi:10.1074/jbc.271.8.4482

Hellqvist, M., Mahlapuu, M., Blixt, A., Enerbäck, S. and Carlsson, P. (1998). The human forkhead protein FREAC-2 contains two functionally redundant activation domains and interacts with TBP and TFIIB. *J. Biol. Chem.* **273**, 23335-23343. doi:10.1074/jbc.273.36.23335

Hosokawa, R., Oka, K., Yamaza, T., Iwata, J., Urata, M., Xu, X., Bringas, P., Jr., Nonaka, K. and Chai, Y. (2010). TGF-β mediated FGF10 signaling in cranial neural crest cells controls development of myogenic progenitor cells through tissue-tissue interactions during tongue morphogenesis. *Dev. Biol.* **341**, 186-195. doi:10.1016/j.ydbio.2010.02.030

Ingham, P. W. and McMahon, A. P. (2001). Hedgehog signaling in animal development: paradigms and principles. *Genes Dev.* **15**, 3059-3087. doi:10.1101/gad.938601
Iwasaki, S.-I. (2002). Evolution of the structure and function of the vertebrate tongue. *J. Anat.* **201**, 1-13. doi:10.1046/j.1469-7580.2002.00073.x
Jeong, J., Mao, J., Tenzen, T., Kottmann, A. H. and McMahon, A. P. (2004). Hedgehog signaling in the neural crest cells regulates the patterning and growth of facial primordia. *Genes Dev.* **18**, 937-951. doi:10.1101/gad.1190304
Jung, H.-S., Oropeza, V. and Thesleff, I. (1999). Shh, Bmp-2, Bmp-4 and Fgf-8 are associated with initiation and patterning of mouse tongue papillae. *Mech. Dev.* **81**, 179-182. doi:10.1016/S0925-4773(98)00234-2
Kapsimali, M. and Barlow, L. A. (2013). Developing a sense of taste. *Semin. Cell Dev. Biol.* **24**, 200-209. doi:10.1016/j.semcdb.2012.11.002
Kaufmann, E. and Knöchel, W. (1996). Five years on the wings of fork head. *Mech. Dev.* **57**, 3-20. doi:10.1016/0925-4773(96)00539-4
Lan, Y. and Jiang, R. (2009). Sonic hedgehog signaling regulates reciprocal epithelial-mesenchymal interactions controlling palatal outgrowth. *Development* **136**, 1387-1396. doi:10.1242/dev.028167
Lan, Y., Kingsley, P. D., Cho, E.-S. and Jiang, R. (2001). Osr2, a new mouse gene related to Drosophila odd-skipped, exhibits dynamic expression patterns during craniofacial, limb, and kidney development. *Mech. Dev.* **107**, 175-179. doi:10.1016/S0925-4773(01)00457-9
Liu, C.-F., Aschbacher-Smith, L., Barthelery, N. J., Dyment, N., Butler, D. and Wylie, C. (2012). Spatial and temporal expression of molecular markers and cell signals during normal development of the mouse patellar tendon. *Tissue Eng. Part A* **18**, 598-608. doi:10.1089/ten.tea.2011.0338
Liu, C.-F., Breidenbach, A., Aschbacher-Smith, L., Butler, D. and Wylie, C. (2013). A role for hedgehog signaling in the differentiation of the insertion site of the patellar tendon in the mouse. *PLoS ONE* **8**, e65411. doi:10.1371/journal.pone.0065411
Long, F., Zhang, X. M., Karp, S., Yang, Y. and McMahon, A. P. (2001). Genetic manipulation of hedgehog signaling in the endochondral skeleton reveals a direct role in the regulation of chondrocyte proliferation. *Development* **128**, 5099-5108. doi:10.1242/dev.128.24.5099
Love, M. I., Huber, W. and Anders, S. (2014). Moderated estimation of fold change and dispersion for RNA-seq data with DESeq2. *Genome Biol.* **15**, 550. doi:10.1186/s13059-014-0550-8
Mahlapuu, M., Pelto-Huikko, M., Aitola, M., Enerbäck, S. and Carlsson, P. (1998). FREAC-1 contains a cell-type-specific transcriptional activation domain and is expressed in epithelial-mesenchymal interfaces. *Dev. Biol.* **202**, 183-195. doi:10.1006/dbio.1998.9010
Mahlapuu, M., Ormestad, M., Enerback, S. and Carlsson, P. (2001). The forkhead transcription factor Foxf1 is required for differentiation of extra-embryonic and lateral plate mesoderm. *Development* **128**, 155-166. doi:10.1242/dev.128.2.155
Martin, J. F., Bradley, A. and Olson, E. N. (1995). The paired-like homeo box gene MHox is required for early events of skeletogenesis in multiple lineages. *Genes Dev.* **9**, 1237-1249. doi:10.1101/gad.9.10.1237
McMahon, A. P., Ingham, P. W. and Tabin, C. J. (2003). Developmental roles and clinical significance of hedgehog signaling. *Curr. Top. Dev. Biol.* **53**, 1-114. doi:10.1016/S0070-2153(03)53002-2
Minoux, M., Holwerda, S., Vitobello, A., Kitazawa, T., Kohler, H., Stadler, M. B. and Rijli, F. M. (2017). Gene bivalency at Polycomb domains regulates cranial neural crest positional identity. *Science* **355**, eaal2913. doi:10.1126/science.aal2913
Muzumdar, M. D., Tasic, B., Miyamichi, K., Li, L. and Luo, L. (2007). A global double-fluorescent Cre reporter mouse. *Genesis* **45**, 593-605. doi:10.1002/dvg.20335
Nassari, S., Duprez, D. and Fournier-Thibault, C. (2017). Non-myogenic contribution to muscle development and homeostasis: the role of connective tissues. *Front. Cell Dev. Biol.* **5**, 22. doi:10.3389/fcell.2017.00022
Okuhara, S., Birjandi, A. A., Adel Al-Lami, H., Sagai, T., Amano, T., Shiroishi, T., Xavier, G. M., Liu, K. J., Cobourne, M. T. and Iseki, S. (2019). Temporospatial sonic hedgehog signalling is essential for neural crest-dependent patterning of the intrinsic tongue musculature. *Development* **146**, dev180075. doi:10.1242/dev.180075
Parada, C. and Chai, Y. (2015). Mandible and tongue development. *Curr. Top. Dev. Biol.* **115**, 31-58. doi:10.1016/bs.ctdb.2015.07.023
Parada, C., Han, D. and Chai, Y. (2012). Molecular and cellular regulatory mechanisms of tongue myogenesis. *J. Dent. Res.* **91**, 528-535. doi:10.1177/0022034511434055
Park, J.-S., Ma, W., O'Brien, L. L., Chung, E., Guo, J.-J., Cheng, J.-G., Valerius, M. T., McMahon, J. A., Wong, W. H. and McMahon, A. P. (2012). Six2 and Wnt regulate self-renewal and commitment of nephron progenitors through shared gene regulatory networks. *Dev. Cell* **23**, 637-651. doi:10.1016/j.devcel.2012.07.008
Peterson, R. S., Lim, L., Ye, H., Zhou, H., Overdier, D. G. and Costa, R. H. (1997). The winged helix transcriptional activator HFH-8 is expressed in the mesoderm of the primitive streak stage of mouse embryos and its cellular derivatives. *Mech. Dev.* **69**, 53-69. doi:10.1016/S0925-4773(97)00153-6
Pryce, B. A., Brent, A. E., Murchison, N. D., Tabin, C. J. and Schweitzer, R. (2007). Generation of transgenic tendon reporters, ScxGFP and ScxAP, using regulatory elements of the scleraxis gene. *Dev. Dyn.* **236**, 1677-1682. doi:10.1002/dvdy.21179
Pryce, B. A., Watson, S. S., Murchison, N. D., Staverosky, J. A., Dünker, N. and Schweitzer, R. (2009). Recruitment and maintenance of tendon progenitors by TGFβ signaling are essential for tendon formation. *Development* **136**, 1351-1361. doi:10.1242/dev.027342
Ren, X., Ustiyan, V., Pradhan, A., Cai, Y., Havrilak, J. A., Bolte, C. S., Shannon, J. M., Kalin, T. V. and Kalinichenko, V. V. (2014). FOXF1 transcription factor is required for formation of embryonic vasculature by regulating VEGF signaling in endothelial cells. *Circ. Res.* **115**, 709-720. doi:10.1161/CIRCRESAHA.115.304382
Riddle, R. D., Johnson, R. L., Laufer, E. and Tabin, C. (1993). Sonic hedgehog mediates the polarizing activity of the ZPA. *Cell* **75**, 1401-1416. doi:10.1016/0092-8674(93)90626-2
Ruest, L.-B., Dager, M., Yanagisawa, H., Charité, J., Hammer, R. E., Olson, E. N., Yanagisawa, M. and Clouthier, D. E. (2003). dHAND-Cre transgenic mice reveal specific potential functions of dHAND during craniofacial development. *Dev. Biol.* **257**, 263-277. doi:10.1016/S0012-1606(03)00068-X
Sawtell, N. M. and Lessard, J. L. (1989). Cellular distribution of smooth muscle actins during mammalian embryogenesis: expression of the α-vascular but not the γ-enteric isoform in differentiating striated myocytes. *J. Cell Biol.* **109**, 2929-2937. doi:10.1083/jcb.109.6.2929
Schwartz, A. G., Long, F. and Thomopoulos, S. (2015). Enthesis fibrocartilage cells originate from a population of Hedgehog-responsive cells modulated by the loading environment. *Development* **142**, 196-206. doi:10.1242/dev.112714
Soriano, P. (1999). Generalized lacZ expression with the ROSA26 Cre reporter strain. *Nat. Genet.* **21**, 70-71. doi:10.1038/5007
Tickle, C. and Towers, M. (2017). Sonic Hedgehog signaling in limb development. *Front. Cell Dev. Biol.* **5**, 14. doi:10.3389/fcell.2017.00014
Xu, J., Liu, H., Park, J.-S., Lan, Y. and Jiang, R. (2014). Osr1 acts downstream of and interacts synergistically with Six2 to maintain nephron progenitor cells during kidney organogenesis. *Development* **141**, 1442-1452. doi:10.1242/dev.103283
Xu, J., Liu, H., Lan, Y., Adam, M., Clouthier, D. E., Potter, S. and Jiang, R. (2019). Hedgehog signaling patterns the oral-aboral axis of the mandibular arch. *eLife* **8**, e40315. doi:10.7554/eLife.40315
Xu, J., Liu, H., Lan, Y., Park, J. S. and Jiang, R. (2020). Genome-wide identification of Foxf2 target genes in palate development. *J. Dent. Res.* **99**, 463-471. doi:10.1177/0022034520904018
Yamane, A., Amano, O. and Slavkin, H. C. (2003). Insulin-like growth factors, hepatocyte growth factor and transforming growth factor-alpha in mouse tongue myogenesis. *Dev. Growth Differ.* **45**, 1-6. doi:10.1046/j.1440-169X.2003.00669.x
Yang, X. M., Vogan, K., Gros, P. and Park, M. (1996). Expression of the met receptor tyrosine kinase in muscle progenitor cells in somites and limbs is absent in Splotch mice. *Development* **122**, 2163-2171. doi:10.1242/dev.122.7.2163
Zhang, Y., Zhao, X., Hu, Y., St Amand, T., Zhang, M., Ramamurthy, R., Qiu, M. and Chen, Y. (1999). Msx1 is required for the induction of Patched by Sonic hedgehog in the mammalian tooth germ. *Dev. Dyn.* **215**, 45-53. doi:10.1002/(SICI)1097-0177(199905)215:1<45::AID-DVDY5>3.0.CO;2-5
Zhang, X. M., Ramalho-Santos, M. and McMahon, A. P. (2001). Smoothened mutants reveal redundant roles for Shh and Ihh signaling including regulation of L/R asymmetry by the mouse node. *Cell* **106**, 781-792. doi:10.1016/S0092-8674(01)00385-3